UNCLASSIFIED

SECURITY CLASSIFICATION OF THIS PAGE

REPORT DOCUMENTATION PAGE

1a. REPORT SECURITY CLASSIFICATION Unclassified	1b. RESTRICTIVE MARKINGS None
2a. SECURITY CLASSIFICATION AUTHORITY	3. DISTRIBUTION/AVAILABILITY OF REPORT Approved for public release; distribution is unlimited.
2b. DECLASSIFICATION/DOWNGRADING SCHEDULE	
4. PERFORMING ORGANIZATION REPORT NUMBER(S) NORDA Technical Note 259	5. MONITORING ORGANIZATION REPORT NUMBER(S) NORDA Technical Note 259
6. NAME OF PERFORMING ORGANIZATION Naval Ocean Research and Development Activity	7a. NAME OF MONITORING ORGANIZATION Naval Ocean Research and Development Activity
6c. ADDRESS (City, State, and ZIP Code) Ocean Science Directorate NSTL, Mississippi 39529-5004	7b. ADDRESS (City, State, and ZIP Code) Ocean Science Directorate NSTL, Mississippi 39529-5004
8a. NAME OF FUNDING/SPONSORING ORGANIZATION Sandia National Laboratories 8b. OFFICE SYMBOL (If applicable)	9. PROCUREMENT INSTRUMENT IDENTIFICATION NUMBER FAO No. 58-5880
8c. ADDRESS (City, State, and ZIP Code) Alburquerque, New Mexico	10. SOURCE OF FUNDING NOS. PROGRAM ELEMENT NO. / PROJECT NO. / TASK NO. / WORK UNIT NO.
11. TITLE (Include Security Classification) Pore Pressure Response to Probe Insertion and Thermal Gradient: ISIMU–II	
12. PERSONAL AUTHOR(S) M. Riggins, P. J. Valent, H. Li, and J. T. Burns	
13a. TYPE OF REPORT Final	13b. TIME COVERED From _____ To _____
14. DATE OF REPORT (Yr., Mo., Day) July 1985	15. PAGE COUNT 80
16. SUPPLEMENTARY NOTATION	
17. COSATI CODES FIELD / GROUP / SUB. GR.	18. SUBJECT TERMS (Continue on reverse if necessary and identify by block number) pore pressure, piezometer, probes, sediment cracking

19. ABSTRACT (Continue on reverse if necessary and identify by block number)

The described experiment and the evaluation of its results were designed to assess the significance of the sediment cracking occurring during piezometer and heater probe insertion, and the influence of the cracking on the subsequent excess pore presure and thermal fields to be measured in the In Situ Heat Transfer Experiment (ISHTE). The ISHTE is part of the Subseabed Disposal Program (SDP) managed by Sandia National Laboratories Albuquerque (SNLA) and funded by the Department of Energy. Observed sediment radial cracking was estimated to penetrate to about one-half penetrator diameter. Measured penetrator insertion pore pressures and excess pore pressure dissipation indicate that sediment cracking has no identifiable influence at the penetration depth of the sensors. Proper prediction of the dissipation of insertion pore pressures was found to require incorporation of a smear factor, accounting for sediment remolding at the piezometer wall. An analytical model to concurrently describe the rise in excess pore pressures due to sediment heating and the pore pressure dissipation radially away from the heat source is described and the results of its application to the experiment data evaluated.

20. DISTRIBUTION/AVAILABILITY OF ABSTRACT UNCLASSIFIED/UNLIMITED ☐ SAME AS RPT. ■ DTIC USERS ☐	21. ABSTRACT SECURITY CLASSIFICATION Unclassified
22a. NAME OF RESPONSIBLE INDIVIDUAL P. J. Valent	22b. TELEPHONE NUMBER (Include Area Code) (601) 688-4621 22c. OFFICE SYMBOL Code 363

DD FORM 1473, 83 APR EDITION OF 1 JAN 73 IS OBSOLETE.

UNCLASSIFIED

SECURITY CLASSIFICATION OF THIS PAGE

NORDA Technical Note 259

Naval Ocean Research and
Development Activity
NSTL, Mississippi 39529

Pore Pressure Response to Probe Insertion and Thermal Gradient: ISIMU–II

Michael Riggins, Philip J. Valent,
Huon Li, John T. Burns
Ocean Science Directorate
Seafloor Geosciences Division

Charles E. Hickox
Sandi National Laboratories
Albuquerque, New Mexico

July 1985

Pore Pressure Response to Probe Insertion and Thermal Gradient: ISIMU-II

by

*Michael Riggins, Philip J. Valent and Huon Li,
Naval Ocean Research and Development Activity,
NSTL, MS

Charles E. Hickox, Sandia National Laboratories, Albuquerque, NM,

and John T. Burns, Naval Ocean Research and Development Activity,
NSTL, MS

sponsored by

Sandia National Laboratories, Albuquerque, NM, under FAO No. 58-5880

November 1984

Naval Ocean Research and Development Activity
NSTL, Mississippi

*Presently Assistant Professor, Colorado School of Mines, Golden, CO

ABSTRACT

The described experiment and the evaluation of its results were designed to assess the significance of the sediment cracking occurring during piezometer and heater probe insertion, and the influence of the cracking on the subsequent excess pore pressure and thermal fields to be measured in the In Situ Heat Transfer Experiment (ISHTE). The ISHTE is part of the Subseabed Disposal Program (SDP) managed by Sandia National Laboratories Albuquerque (SNLA) and funded by the Department of Energy. Observed sediment radial cracking was estimated to penetrate to about one-half penetrator diameter. Measured penetrator insertion pore pressures and excess pore pressure dissipation indicate that sediment cracking has no identifiable influence at the penetration depth of the sensors. Proper prediction of the dissipation of insertion pore pressures was found to require incorporation of a smear factor, accounting for sediment remolding at the piezometer wall. An analytical model to concurrently describe the rise in excess pore pressures due to sediment heating and the pore pressure dissipation radially away from the heat source is described and the results of its application to the experiment data evaluated.

1.0 INTRODUCTION

1.1 Purpose

This report presents the results of a laboratory simulation, conducted at atmospheric pressure, of the planned In Situ Heat Transfer Experiment (ISHTE). The purposes of this laboratory simulation were to:

a) determine the depth of sediment cracking resulting from the insertion of probes into the sediment,

b) measure and evaluate the excess pore pressures generated during the insertion of probes into the sediment, and

c) measure and evaluate the excess pore pressures generated by the application of a thermal gradient in the sediment.

1.2 Background

The Subseabed Disposal Program (SDP) is studying the feasibility of sequestering high level nuclear waste in fine-grained deep-sea formations of the world ocean basins (Hollister et al., 1981). The ISHTE field test will provide data on the thermal, fluid dynamic and thermochemical response of in-situ seabed sediment for use in verification of laboratory experimental approaches and computer models of waste/sediment thermal interaction. During the

test, the sediment response will be studied by conducting the following series of measurements (Percival, 1983):

a) Thermal conductivity;

b) Temperature, to develop a "picture" of the thermal field;

c) Excess pore water pressure;

d) Ion migration;

e) Sampling of pore water constituents;

f) Vane shear strength; and

g) Permeabilities and undrained shear strengths of core samples.

These tests will be performed from the ISHTE platform; both before and after implant of an isotopic heat source.

To prepare for design of the ISHTE experiment, the ISHTE Simulation Experiment (ISIMU) was performed on a 0.287:1 scale model of the platform. The first test (ISIMU-I) was conducted from November 2 thru December 15, 1981, at the David Taylor Naval Ship Research and Development Center (Miller et al., 1982). In ISIMU-I, the various sensors were implanted in a re-constituted illitic "red clay" sediment (Silva et al., 1983). The sensors and sediment sample were placed in a large pressure vessel and pressurized to 55 MPa, to simulate the deep sea environment, for a one month period. The primary objectives of the experiment included (Percival, 1983):

a) Determination of the transient temperature distribution in the sediment;

b) Measurements of the thermal conductivity of the sediment;

c) Measurements of transient pore pressures;

d) Measurements of transient sediment response to the applied pressure;

e) Measurements of the sediment shear strength;

f) Studies of the pore water chemistry; and

g) Post-test studies of the sediment mineralogy, chemistry, and structure.

ISIMU-I produced two unexpected results. First, for a given heater power level, the maximum temperature of the surrounding sediment was approximately 25 percent lower than that predicted based on pretest measurements of the sediment properties (Percival, 1983). The second unexpected result was that the excess pore pressure developed on insertion of the pore pressure probe in the near-field (15 mm from heating element) was approximately one half that of the far-field pore pressure probe (342 mm from heating element) (Bennett et al., in press). Cracking of the sediment surface was noted to accompany the insertion of the Electric Heat Source (EHS), the pore pressure probes, and the geochemistry sampler. These sediment cracks were hypothesized to penetrate to the vicinity of the heater source and the pore pressure sensors and

to be responsible for the unexpected temperature and excess pore pressure dissipation results. ISIMU-I also produced information on the impact of sediment heating on the excess pore pressures. Upon heating, the near-field piezometer displayed a very short term lag in response (<4 min) followed by a short term (<40 min) increase in pressure with a subsequent long-term (~90 hrs) exponential decrease in pressure. The far-field piezometer showed a significant short term lag (~8 hrs) followed by a long term (~120 hr) pressure increase. The two pressures for the very long term (> 120 hrs) leveled off at approximately the same values.

ISIMU-I then, while providing answers to many questions, also left questions unanswered and raised new ones. This report describes a follow-up experiment designed to help resolve some of the questions remaining after ISIMU-I.

1.3 Approach

To further evaluate the ISIMU-I results, an additional simulation experiment (ISIMU-II) was performed. This test was conducted from April 2 to April 5, 1984, at Sandia National Laboratories in Albuquerque (SNLA). Since only the thermal and pore pressure response characteristics of the sediment were of interest, ISIMU-II did not involve pressurization to the deep-sea environment or the same level of instrumentation as ISIMU-I. Two pore pressure probes were placed within 15 mm of a heating probe in a 0.46 m diameter tank filled with re-constituted illite sediment (the same sediment used in ISIMU-I). The heater probe and the tank walls were instrumented with thermocouples. Pore pressures were monitored

during the individual probe insertions, and during subsequent heating.

This report, describing ISIMU-II and its results, is arranged in four sections. The first section describes the test arrangement and data reduction. The next section discusses the development of models to predict: (1) the excess pore water pressure dissipation following probe insertion and (2) the excess pore pressure build-up due to thermal effects. The third section presents the results of the experiment and the application of the proposed prediction models. The last section summarizes the study.

2.0 TEST ARRANGEMENT

2.1 Sediment Sample Preparation

The sediment sample used in the ISIMU-II experiment was prepared at SNLA. The sediment used was the same pelagic clay from MPG-I, of primarily illitic composition, used in the ISIMU-I experiment. This material had been shipped from NSRDC, Annapolis, MD, to SNLA in 55-gallon drums and stored. This material was reconstituted in a plaster mixer into a thick slurry state and poured into the sediment tank in 0.15 m layers. Vacuum was applied after each layer had been placed to de-air the material. The sediment tank used in ISIMU-II was a glass cylinder with a sand filter at the bottom (Figure 1), burlap fabric filters on the sides, and a fiber filter sheeting between the sediment and the burlap to limit clogging of the burlap. The slurry sample was loaded in increments, using deadweights, to duplicate the consolidation state

achieved in ISIMU-I. The resulting sample was 0.43 m (17 in) in diameter and 0.71 m (28 in) in height.

2.2 Condition of Sample at Testing

Cores were taken at the conclusion of the test and water contents and miniature vane shear strengths measured on those cores. The results of these tests on the cores are reported and discussed later in this report. Tests on the peripheral cores show the sediment sample to be of fairly uniform water content (average 88.0 percent) and undrained shear strength (average 4.1 kPa) with depth. Sufficient samples and tests were not conducted to provide for evaluating the variability in water content and strength across the diameter of the test tank; however, prior experience with this sample preparation technique for ISIMU-I suggests this variation will not be significant (Silva et al., 1983).

2.3 Pore Pressure Probes

The pore pressure probes are of the same design as those used in ISIMU-I and to be used on the ISHTE platform. The probe sensing element is mounted on a 7.94 mm (5/16 in.) diameter titanium tube about 1 m in length. The probe tip is a cone 100 mm in length and 7.9 mm diameter at its base (5.3 degree cone angle), designed to induce two-dimensional, or lateral, deformation during penetration into the sediments (Bennett et al., 1981 and in press). The excess pore pressures are sensed at a 13 mm long (1/2 in.) cylindrical porous corundum stone located 160 mm from the probe tip. The pore pressures sensed at this porous stone are transmitted through the

titanium tube to a variable reluctance differential pressure transducer located 1 m above the porous stone (Bennett et al., 1980, 1983, and in press).

2.4 Insertion Experiment

ISIMU-II was intended to duplicate the heater probe and near-field pore pressure probe insertions performed in ISIMU-I. In ISIMU-I, the near-field pore pressure probe was positioned 15 mm, wall-to-wall, from the heater probe, and it had been planned to position the porous stone at the same elevation as the center of the heating element. However, post-test inspection revealed that the near-field piezometer had not attained the planned penetration, but had stopped 101 mm short (Miller et al., 1982). Therefore, in order to duplicate the original test conditions, the porous stones of the probes used in ISIMU-II were both positioned 101 mm above the mid-plane of the heat source (Figure 2).

The original plan of ISIMU-II called for installation of the heater probe at the center of the tank. A 100 mm (4-in.) thick block of Teflon, with 3 bored guide holes for the heater and two pore pressure probes, was fixed over the top of the tank. The first piezometer was saturated by first immersing the probe tip including porous stone in the 150 mm (5-3/4 in.) of water overlying the sediment surface. A partial vacuum was then applied to the positive bleed port of the transducer, standing some 0.7 m above the water surface, and water thus drawn up into the transducer to saturate the system. On installation, this first probe exhibited a response time of 3 minutes, which was considered to be too long for a properly

saturated pore pressure probe. This probe was removed the following day and replaced with a dummy, pointed, 7.94 mm (5/16-in.) diameter stainless steel rod, to fill the hole.

To minimize the disturbance and the discontinuity of the dummy rod, the Teflon guide block was reoriented 90 degrees and the proposed location of the heater moved 44 mm (1-3/4 in.) off tank center. For the first pore pressure probe, denoted as P-3, the saturated porous stone and cone tip were attached under the water surface to facilitate system de-airing. A saturation sleeve was installed over the porous stone and water was driven through the sleeve and stone and up the probe tube/shaft to fill/saturate the transducer positive side. This probe was then inserted over a period of 8 seconds and exhibited a response time of 40 seconds to peak insertion pressure, which was considered indicative of a satisfactorily saturated system. The excess pore pressures generated by this pore pressure probe were allowed to dissipate for 156 minutes (analysis of the data shows that 95% dissipation occurred at about 90 minutes). The heater (23.7 mm diameter) was then inserted, again guided by the Teflon block, with the heater wall 15 mm from the pore pressure probe wall (Figure 2). Insertion pressures generated by the unpowered heater probe were allowed to dissipate over 19 hours. The second piezometer probe, designated P-2, was saturated in the same manner as P-3, was installed on the opposite side of the heater from P-3 (Figure 2), also exhibited a 40 sec response time to peak insertion pressure, and was allowed 118 minutes for excess pore pressure dissipation.

2.5 Heater Experiment

Seven thermocouples were located in the sediment filled tank in the positions noted in Figure 2. The number and location of each are as follows:

0. - At the tank wall in the sediment, 280 mm below mudline.
1. - On the heater element, 50 mm below mid-plane.
2. - On the heater element, at mid-plane.
3. - On the heater element, 50 mm above mid-plane.
4. - On the heater element, at mid-plane.
5. - At the tank surface, in air, at ambient temperature.
6. - At the tank wall in the sediment, 280 mm below mudline.

After the excess pore pressures from the insertion of piezometer probe P-2 had dissipated, the heater probe element was energized to about 29.4 watts. This power input was maintained for 251 minutes while developing/dissipating excess pore pressures were monitored on pore pressure probes P-3 and P-2. The heater response portion of the experiment was terminated after 251 minutes due to a power failure. Even though the power was restored within 5 minutes, the hiatus in the energized condition was sufficient to adversely impact the analysis of subsequent data (given the existing analytical models) therefore continuing the experiment after the power failure was without merit. However, sufficient data were collected during the 251 minutes, before the power failure, to make the heater response portion of the experiment meaningful.

2.6 Data Reduction

The test data were recorded using a Fluke data logger and a Hewlett-Packard strip chart recorder. The raw data consisted of the time (days, hours, minutes, and seconds) at which the measurements were made, voltage output for each transducer and temperature indicated by each thermocouple. A tabulation of the data is given in Addendum I.

The data were stored on a floppy disc and reduced using a Hewlett-Packard model 85 computer. The times were adjusted to reflect the total elapsed time since the beginning of the test. The voltages were transformed to pressures using the following equations:

for probe P-3,

$$\text{Pressure (psi)} = 0.0111 + 3.9982 \star (\text{volts} + 0.1505) \quad . \ . \ . \quad (1)$$

and for probe P-2,

$$\text{Pressure (psi)} = 0.0391 + 3.9950 \star (\text{volts} + 0.1071) \quad . \ . \ . \quad (2)$$

The values 0.1505 and 0.1071 volts represent the zero offset correction for the probes inserted in the sediment.

The variation in pressure for the two probes over the duration of the test are shown in Figure 3. The pressures for the individual test events are shown in Figures 4 to 7. It should be noted that

the small peak at the end of Figure 4 is an actual event. A lucite collar on the pore pressure probe (P-3) had to be removed in order to provide clearance for insertion of the heater probe. During removal of this collar the probe P-3 was twisted gently and only slightly. Disturbance of the sediment during this slight movement resulted in a 0.31 kPa (0.045 psi) excess pore pressure. The beginning of Event 2, the heater probe insertion, was postponed about 18 minutes to allow for dissipation of the excess pore pressure generated by the disturbance.

In addition, it should be noted that the initial pore pressure drop shown in Figure 7 is a result of the time lag between the initiation of heating and the pore pressure response at the probe 15 mm away. The pressure drop is a result of pore pressure dissipation carried over from Event 3 (second pore pressure probe insertion). A complete listing of the reduced data is given in Addendum II.

3.0 GENERAL THEORY AND MODEL DEVELOPMENT

3.1 Pore Pressure Dissipation

Several theories (Acar et al., 1982; Baligh and Levadoux, 1980; Levadoux and Baligh, 1980; Randolph et al., 1979; Soderberg, 1962; Torstensson, 1977; Tumay and Acar, 1984, and Wroth et al., 1979) have been advanced pertaining to the dissipation of excess pore water pressures induced by the expansion of a cylindrical cavity. The governing differential equation in two dimensions is as follows:

$$\frac{\partial u}{\partial t} = c_h \left[\frac{1}{r} \frac{\partial}{\partial r} \left(r \frac{\partial u}{\partial r} \right) \right] \qquad \ldots\ldots\ldots\ldots\ldots\ldots (3)$$

where,

u = excess pore pressure,

t = time,

r = radial distance, and

c_h = horizontal coefficient of consolidation.

Due to the usual lack of horizontal coefficient of consolidation data, c_h, the constant c_h is usually replaced by the coefficient of vertical consolidation, c_v; which is normally equal to or less than c_h (Soderberg, 1962). The coefficient of vertical consolidation is defined as:

$$c_v = \frac{k\ (1 + e)}{a_v\ \gamma} \qquad \ldots\ldots\ldots\ldots\ldots\ldots\ldots\ldots \quad (4)$$

where,

k = permeability

e = void ratio,

a_v = coefficient of vertical compressibility, and

γ = unit weight of water

The most commonly used method of solving Equation (3) involves expressing the excess pore pressure in terms of a dimensionless dissipation factor U (u/u_{max}) which then becomes a function of a dimensionless time factor expressed as,

$$T_r = \frac{c_h t}{r_o^2} \qquad \ldots\ldots\ldots\ldots\ldots\ldots\ldots\ldots \quad (5)$$

where,

r_o = radius of the embedded cylinder.

The functional relationship between U and T_r depends primarily on how one characterizes the sediment. Past pore pressure probe studies (e.g., Bennett et al., 1984) have relied on the solutions of Soderberg (1962) and Randolph et al., (1979), which were developed for a foundation pile embedded in either: (a) an elasto-plastic medium or (b) a viscous medium. Using the general form of the solution one can obtain T_r values for various levels of dissipation. The most common procedure uses the fifty percent dissipation level which yields a T_r approximately equal to one. Then Equation (5) can be rewritten as,

$$c_h = \frac{r_o^2 \, T_{r50}}{t_{50}} \quad \ldots\ldots\ldots\ldots\ldots\ldots\ldots\ldots\ldots\ldots (6)$$

where t_{50} represents the actual time at which fifty percent dissipation has occurred, as obtained from a U versus log t plot.

With c_h thus determined from Equation (6), U can be defined in terms of an exponentially decreasing function of T_r. This method normally employs a series (Scott, 1963); however, for the sake of simplicity only the first term in the series will be used. In addition, the expression is written in terms of real time as,

$$\frac{u}{u_{max}} = e^{-\beta t} \quad \ldots\ldots\ldots\ldots\ldots\ldots\ldots\ldots\ldots\ldots (7)$$

where,

$$\beta = \frac{c_h}{m r_o^2} \quad \ldots\ldots\ldots\ldots\ldots\ldots\ldots\ldots\ldots\ldots (8)$$

The value of m depends upon the assumptions used in the theory. Scott (1963) introduced the concept of a "smear" factor for which the parameter m is used to reflect the reduction in permeability at the boundary due to remolding. This concept can be used to account for the disturbance between the probe and the surrounding sediment.

3.2 Thermally Induced Pore Pressures

An induced thermal field can have a pronounced effect on the pore pressure response of a sediment. If the temperature increase is rapid, a significant excess positive pore pressure can develop, due to the greater volumetric expansion of the sediment pore water than that of the mineral solids. The thermally induced pore pressure change for the undrained condition can be expressed in terms of the following equation developed by Mitchell (1976):

$$\Delta u = \frac{\Delta T}{m_{vs}} \left[n(\alpha_s - \alpha_w) + \alpha_{st} \right] \quad \ldots\ldots\ldots\ldots\ldots\ldots \quad (9)$$

where,

ΔT = temperature change,

m_{vs} = coefficient of compressibility of the soil structure from the rebound-reloading curve of a one-dimensional consolidation test,

n = porosity,

α_s = thermal coefficient of volumetric expansion for the mineral solids,

α_w = thermal coefficient of expansion of the pore water, and

α_{st} = thermal coefficient of expansion for the soil structure.

In considering the problem of the pore pressures at the pore pressure probe, one can think of the transient thermal flux, i.e., when the temperature "front" first contacts the probe, as being of

the undrained case. However, in the long term case, as temperatures attain the "steady state" condition significant spatial temperature gradients form in the sediment medium (Percival, 1983). These gradients result in a dissipation of the excess pore water pressure in the direction of decreasing temperature, i.e., to zones of lower pore water pressures. Therefore, in developing a model for the thermally induced pore pressures at the probe one must consider not only the gain in pore pressure with respect to temperature and time, but also the loss. In lieu of a more rigorous dissipation model involving temperature, the proposed model will involve a superposition of the pore pressure gain and loss, viz.;

$$u = u_{gain} - u_{loss} \quad \ldots\ldots\ldots\ldots\ldots\ldots \quad (10)$$

where u_{gain} and u_{loss} are represented by Equations (9) and (7), respectively. The physical significance of u_{gain} and u_{loss}, as a function of time, can be observed from Figure 8 and the following time sequence:

$$t = 1: \quad u_{gain} = \Delta u_1$$

$$u_{loss} = \Delta u_1 - \Delta u_1 e^{-\bar{\beta}(t_1 - t_1)}$$

$$t = 2: \quad u_{gain} = \Delta u_1 + \Delta u_2$$

$$u_{loss} = (\Delta u_1 - \Delta u_1 e^{-\bar{\beta}(t_2 - t_1)}) + (\Delta u_2 - \Delta u_2 e^{-\bar{\beta}(t_2 - t_2)})$$

$$t = 3: \quad u_{gain} = \Delta u_1 + \Delta u_2 + \Delta u_3$$

$$u_{loss} = (\Delta u_1 - \Delta u_1 e^{-\bar{\beta}(t_3 - t_1)}) + (\Delta u_2 - \Delta u_2 e^{-\bar{\beta}(t_3 - t_2)}) + (\Delta u_3 - \Delta u_3 e^{-\bar{\beta}(t_3 - t_3)})$$

hence the following series for any time, k:

$$u_{gain} = \sum_{i=1}^{k} \Delta u_i \quad \ldots\ldots\ldots\ldots\ldots\ldots \quad (11a)$$

$$u_{loss} = \sum_{i=1}^{k} \Delta u_i - \sum_{i=1}^{k} \Delta u_i e^{-\bar{\beta}(t_k - t_i)} \quad \ldots\ldots\ldots \quad (11b)$$

Substituting Equations (11a and 11b) into Equation (10) and cancelling the like terms yields the total excess pore pressure at time t_k:

$$u_k = \sum_{i=1}^{k} \Delta u_i \, e^{-\bar{\beta}(t_k - t_i)} \quad \ldots\ldots\ldots\ldots\ldots\ldots \quad (12)$$

It should be noted that in the above formulation, Δu was used in place of u_{max} in Equation (7). This substitution is physically correct in that Δu represents the maximum pore pressure being dissipated for a <u>specific</u> time increment. Thus, Equation (12) can account for thermally induced pore pressures, as well as the time dependent dissipation of these pore pressures.

Note here that the coefficient $\bar{\beta}$ is not the same as the coefficient β defined in Equation (8). The coefficient β describes

the excess pore pressure dissipation at the surface of the piezometer probe and/or heater probe: β describes dissipation radially away from the cylindrical surface of radius r_o. However, during Event 4, that period with the heater turned on, the pore pressure field radially around the piezometer probes is quite non-symmetric and probably not described by Equation (8). The form of the dissipation function, Equation (7), was assumed to remain reasonable, and a new coefficient, $\bar{\beta}$, adopted to describe the dissipation performance at the piezometer resulting from heater heating. A function for $\bar{\beta}$ has not been identified.

4.0 TEST RESULTS AND MODEL VERIFICATION

4.1 Sediment Cracking

One purpose of the ISIMU-II experiment was to estimate the depth of sediment cracking resulting from probe insertion and to assess the impact of this cracking on the excess pore pressure dissipation and on the thermal field. Insertion of the pore pressure probes and the heater probe did result in cracking of the sediment surface. Radial cracks occurred at 30-60^{o} spacing around each probe extending outward to about 2-1/2 probe diameters. These cracks appeared to extend to a sediment depth of about one-half probe diameter. The crack pattern suggests an outward displacement of shallow, pie-shaped wedges of sediment during the initial stages of penetration followed by a less-obvious heave of the local area during continued penetration. The shallowness of the crack system suggests that it will have a negligible influence on the excess pore pressure dissipation and temperature gradient in the vicinity of the

heat source and the pore pressure sensors. The similar dissipation responses of the two piezometers, one installed before the heater, the other after, demonstrates that cracking due to heater installation has not measureably influenced the response of the second piezometer, P-2.

4.2 Pore Pressure Dissipation

This section will deal with application of the theory developed in Section 3.1 to data presented in Section 2.6. In order to determine the horizontal coefficient of consolidation, c_h, it is necessary to plot the data shown in Figures 4, 5, and 6 on a semi-log plot to evaluate t_{100} and then t_{50} (c.f. Equation (6)). The excess pore pressure data were first normalized by dividing by the maximum observed pore pressure value. These data are plotted against log time as shown in Figures 9 and 10 for pore pressure probes P-3 and P-2, respectively. The tests were interrupted at 95 to 98 percent dissipation; therefore, a lower, asymtotic value, i.e., complete dissipation of excess pore water pressures, was not attained. Thus, a lower bound value was interpreted and is shown as the coarse dashed lines in Figures 9 and 10. The value of t_{50} corresponds to the time at which u/u_{max} is slightly greater than 0.5. An exact value of 0.5 was not used since the lower asymptote did not reach 0.0. The t_{50} times are 8.3 and 11.4 minutes for probes P-3 and P-2, respectively. The c_h values obtained from Equation (6) using a probe radius of 0.4 cm are 3.21×10^{-4} and 2.34×10^{-4} cm^2/sec for the respective probes.

Figure 11 is the same type of plot, with the exception that it is for the excess pore pressure dissipation at probe P-3 due to the insertion of the heater probe. The t_{50} time for this event, measured at probe P-3, is 53 minutes as compared to t_{50} times of 8 and 11 minutes for the probe insertions. The longer dissipation time for the heater probe insertion is due primarily to the larger cross-sectional area of the heater probe as compared to the area of the pore pressure probes, with dissipation time at the probe surface being directly proportional to the probe radius squared (from Equation (6)). Further, the t_{50} measured at the pore pressure probe is somewhat longer than the t_{50} that would be measured at the heater probe surface because the dissipation rate decreases as one moves away from the probe surface. An additional point of interest is the prediction that the pore pressure decreases inversely with the radial distance away from the probe (Soderberg, 1962), viz.;

$$u_i = u_o \left(\frac{r_o}{r_o + r_i} \right) \quad \ldots\ldots\ldots\ldots\ldots\ldots\ldots\ldots\ldots (13)$$

where

u_i = excess pore pressure in the sediment at a radial distance r_i from the probe,

u_o = excess pore pressure at the probe of radius r_o

Assuming the maximum excess pore pressure generated during heater probe insertion to be the same as that resulting from the insertion of probe P-3 (11.6 kPa or 1.69 psi), one obtains a predicted value of 5.2 kPa (0.75 psi) at probe P-3 due to heater insertion (using r_o = 12 and r_i = 15 mm). (The above statement assumes that the

change in tip shape, very sharp (pore pressure probe) versus blunt (heater probe) and the change in probe diameter from 7.9 mm to 23.7 mm, have no influence on the excess pore pressure generated during insertion. This predicted value compares favorably with the observed value of 5.8 kPa (0.84 psi). The predicted pressure response at probe P-3 due to the insertion of P-2 is 0.69 kPa (0.10 psi) (using r_o = 4 and r_i = 54 mm) as compared to the observed value of 0.97 kPa (0.14 psi). This comparison ignores the influence of the heater probe, located between the pore pressure probes, on the generated excess pore pressure at P-3.

The above c_h values are used in the dissipation model (Equation (7), assuming m = 1) to predict the dissipation rates shown in Figures 12 and 13 for probes P-3 and P-2, respectively. Also shown in these figures is the least squares exponential curve fit to the data ("*" represents data point). The fit is less than ideal, because the intercept value is forced to be unity, leaving only one parameter (the slope) to be evaluated. The important point to note in Figures 12 and 13 is the very close agreement between the predicted and observed values for the short term (< 5 minutes) behavior. However, in terms of medium to long-term behavior the two curves differ considerably, with the predicted curve showing a much higher dissipation rate. Between the predicted and least squares curves the latter will be considered the more correct in predicting the overall dissipation behavior. Therefore, it becomes necessary to "slow down" the dissipation rate as calculated from Equation (7). This can be achieved through the use of the m value in Equation (8). Figures 14 and 15 show the effects of the m parameter in shifting the predicted curves for probes P-3 and P-2, respectively. The

corresponding m values which resulted in curves closest to the least squares curves are 4.6 and 2.3 for the respective probes. Thus, of the two probes, the dissipation curve for probe P-3 is affected to a greater extent (higher m value) due to insertion. This finding is consistent since P-3 was inserted in "virgin" sediment, whereas, P-2 was inserted in sediment disturbed by the prior insertion of the heater probe.

4.3 Thermally Induced Pore Pressures

The thermally induced excess pore pressures at probes P-3 and P-2 were previously shown in Figure 7. The salient features to be noted from this figure are as follows:

1) the initial 4 minute lag in the pore pressure response,
2) the significant pore pressure decay for times greater than 75 to 100 minutes,
3) the reduced pore pressure response of probe P-2, and
4) the hyperbolic shape of the initial portion of the curves.

The first factor can be directly attributed to the thermal diffusivity of the sediment. The same 4 minute response lag was observed during the ISIMU-I simulation (see Section 1.2). Shifting the curves toward the origin compensates for this factor. The second and third factors are a result of the previous insertion event. Figure 3 clearly shows that pore pressure dissipation during this event had not attained the asymptotic minimum prior to heater "turn-on". Thus, the previous dissipation history must be taken into account. This is achieved by fitting a least squares

exponential curve to the "tail" portion of the curves shown in Figure 6. The correction is added to the original data as is shown in Figures 16 and 17 for probes P-3 and P-2, respectively. The fourth factor is a result of the rate of temperature increase as described by Equation (9). Equation (9) predicts the rate of pore pressure build-up to be directly related to the rate of temperature change. The temperature-time curves, as recorded by thermocouples located on the heater probe, are shown in Figure 18. One observes from this figure the hyperbolic shape of the curves. The actual temperature-time relationship at the piezometer probes was not recorded. However, the thermocouples at the tank wall, 200 mm from the probes, recorded no significant temperature change. Therefore, the actual heating rate must lie somewhere between that shown in Figure 18 and zero. Since the actual curve is not known, the hyperbolic form will be used with assumed parameters.

The hyperbolic relationship is used to calculate the change in temperature for a unit time step which is then substituted into Equation (9) to determine the rate of pore pressure increase. As mentioned in Section 3.2, the pore pressure increase is affected by dissipation into the surrounding sediment, therefore, the unit pore pressure increase must be substituted into Equation (12) and summed over the entire record to obtain the actual pore pressure response. This response is shown in Figures 19 and 20 for probes P-3 and P-2, respectively. In these figures an asterisk, "*", represents corrected data, as described previously, "+" represents the thermally induced pore pressures as obtained from the assumed temperature-time relationship and Equation (9), and "0" represents the predicted pore pressure build-up using the thermally induced

pore pressure data and Equation (12). For this calculation, as a first approximation, the coefficient $\bar{\beta}$ was assumed equal in value to the coefficient β from Equation (8). The fit of prediction to measured data shown in Figures 19 and 20 was achieved without further adjustment to the value of $\bar{\beta}$. The computer program "MENUDO" used to create these figures is given in Addendum III. The program listing gives the typical values for the sediment structural properties, as well as, the thermal properties of illite (Bennett et al., 1984; Mitchell, 1976; and Silva et al., 1982).

The authors note that much work remains before the temperature-pore pressure response model described herein is accepted as a reliable, effective model. The present model uses a number of soil behavior parameters, e.g., c_v, c_h, m_v, at stress and temperature levels where these behavior parameters are only vaguely understood. Back-calculations of the sediment temperature at the piezometer yield calculated temperatures ranging from one order of magnitude higher to one order of magnitude lower than the measured temperatures at the heater surface, all for reasonable assumptions for input parameter values. Continued effort is required to improve our understanding of the temperature-excess pore pressure generation-dissipation phenomena to the working level.

4.4 Sample Evaluation

After completion of the test program, Dr. Les Shepherd, of Sandia National Laboratories, obtained push cores of the tank sediment near the periphery of the tank in sediment believed least disturbed during the experiment. These peripheral core tubes were

inserted before any of the test probes were withdrawn to minimize possible lateral deformations and disturbance of the sediment during coring. The peripheral cores and probes were then withdrawn and the area of the heater probe was then over-cored. Two of the peripheral cores and the heater overcore were then tested at SNL, and one peripheral core transported as handcarried luggage, was tested at NORDA.

Water contents measured on two cores tested at SNL (without transportation) show the water content to be reasonably constant with depth, varying from 85 to 90 percent with an average for the two cores of 87.6 percent (Figure 21). Water contents on the one core tested at NORDA, after transport by plane and auto, were essentially the same ranging from 87 to 90 percent with an average of 88.8 percent. The water contents measured on the sediments adjacent to the heater probe (sampled by the over-core and tested at SNL) were 2 to 3 percent below the water contents measured in the peripheral cores. These lower water contents may be due to drying during the delay between splitting the core for radiography and subsampling for water content. The water content at the mid-point of the heater element (0.25 m) was measured as 6 to 7 percent below the water content values at 0.20 and 0.30 m (Figure 21). This low value may reflect a thermally-induced consolidation effect (Shephard, 1984).

Radiographic examination of the over-core was performed in order to look for sediment cracking resulting from heater probe insertion. The results of this examination were inconclusive. Cracks developed when the 0.13 m (5 in.) diameter over-core was

split making it very difficult to differentiate between probe implant cracks and core splitting cracks (Shephard, 1984).

The undrained shear strength measured by the miniature vane was noted to be reasonably consistent in the peripheral core tested at SNL, averaging about 4.1 kPa (Figure 22). The core tested at NORDA, after plane and auto transport, reflected a decrease in vane strength with depth from 4.3 kPa near the top to 2.8 kPa near the bottom, probably reflecting sediment disturbance due to transport. Sediment sensitivities as measured by the vane are 4 and greater.

4.5 Strength Prediction from Insertion Pore Pressures

If the sediment is assumed to be properly modeled as an elastic perfectly plastic material, then the maximum excess pore pressure at the probe surface is given by Randolph et al. (1979) as:

$$u_{imax} = s_u \ln (G/s_u) \quad (14)$$

Esrig et al. (1977), noting that the ratio G/s_u can often be predicted based on soil type, suggested a value of 6 for the factor $\ln(G/s_u)$ in Equation (14), for lean inorganic soils of moderate to high sensitivity, resulting in:

$$u_{imax} = s_u \times 6 \quad (15)$$

In ISIMU-II, piezometer probe P-3 measured on insertion-induced excess pore pressure of 11.6 kPa, and vane shear strengths measured

at SNLA on a peripheral core were 4.03 kPa near the piezometer sensor elevation. The resulting pressure-to-strength ratio is:

$$u_{imax}/s_u = 11.6/4.03 = 2.9 \sim 3 \quad (16)$$

This low value of the u_{imax}/s_u ratio is measured on a sample of reconstituted sediment, and, therefore, it is not considered highly significant.

5.0 SUMMARY AND CONCLUSIONS

The surficial sediment crack pattern observed in the ISIMU-II experiment does not suggest significant penetration of the cracks to a depth where the excess pore pressure and heat dissipation might be measureably altered by the cracking. The measured similar insertion and dissipation excess pore pressure histories for the two piezometers, one inserted before the heater probe insertion, the other inserted after, lends support to this position.

The ISIMU-II simulation involved the collection and analysis of data pertaining to induced excess pore water pressure build-up and subsequent dissipation as a result of probe insertion and thermal effects. The rate of dissipation predicted is dependent upon material properties as well as the dissipation model used. The horizontal coefficients of consolidation, c_h, obtained using Soderberg's (1962) method, were found to be consistent with the ISIMU-I results, as well as with oedometer test results (Silva et al., 1982). The c_h values were used in a first order exponentially decreasing dissipation function and found to model short term

behavior. However, the same function when considered in terms of long-term performance predicted a significantly higher dissipation rate. The predicted behavior was "slowed down" using Scott's (1963) "smear" factor in such a fashion as to agree with a least-squares approximation to the data.

The thermally induced pore pressures were modeled using Mitchell's (1976) equation. This expression involves the change in pore water pressure as a function of temperature change and thermal properties of the sediment. The actual rate of temperature change at the probe was not known; however, these data were available for the heating element and container walls. Therefore, the general shape of the curve was known with the parameters defining the curve assumed a priori. The thermally induced pore pressure model was combined with the dissipation model into a single expression, with the former serving as a forcing function for the gain in pore pressure and the latter as a loss term. The proposed equation was found to be a good model in predicting the observed thermally induced pore pressure response.

The temperature increase calculated from the temperature-excess pore pressure model was found to be significantly different than that which would have been predicted from ISIMU-I results. Possible causes for this discrepancy are as follows:

a) Improper prediction of the overall behavior of the sediment by the first order dissipation model,
b) Excessive "slowing down" of the dissipation model resulting in a lower dissipation rate,

c) An over estimate of the thermally induced pore pressures due to errors in the selection of thermal coefficients,

d) Differing heating rates and temperatures between ISIMU-I and ISIMU-II simulations,

e) Differences in the thermal properties and response characteristics of the pore pressure probes, and

f) A change in material properties as a function of temperature, namely, changes in c_h.

6.0 ACKNOWLEDGMENTS

The authors thank Drs. C. Mark Percival, Joel Lipkin, Les E. Shephard, and David F. McTique, all of Sandia National Laboratories, for their assistance during conduct of the experiment. We also thank Dr. Richard H. Bennett and Mr. Douglas N. Lambert, Naval Ocean Research and Development Activity (NORDA) for their review of the manuscript. The efforts of Ms. Dianne Morris (typing) and Ms. F. Lee Nastav (illustrations), NORDA, are gratefully acknowledged. The subject work was completed under Federal Agency Order 58-5880 issued by Sandia National Laboratories, 23 February 1984. Prof. Riggins participation in the analytical model development, data analysis, and documentation was supported by the U.S. Navy-ASEE Summer Faculty Research Program.

7.0 REFERENCES

Acar, Y. B., M. T. Tumay, and A. Chan, 1982. Interpretation of the Dissipation of Penetration Pore Pressures, Proceedings from the International Symposium on Numerical Models in Geomechanics, Zurich, Switzerland, pp 353-358.

Baligh, M. M. and J. M. Levadoux, 1980. Pore Pressure Dissipation after Cone Penetration, MIT Sea Grant Report No. 80-13, 368 p.

Bennett, R. H., J. T. Burns, and D. N. Lambert, 1981. Design and Development of a Deep-Water Piezometer for the Sandia Disposal Program, Subseabed Disposal Program Annual Report: January to December 1980, V. II Appendices (P.I. Progress Reports), Kennetth R. Hinga, Editor, Sandia National Laboratories, Albuquerque, NM, pp 897-904.

Bennett, R. H., J. T. Burns, J. Lipkin, and C. M. Percival, 1983. Piezometer Probe Technology for Geotechnical Investigations in Coastal and Deep-Ocean Environments, Transactions of the 12th Transducer Workshop, Melbourne, FL, 32 pp.

Bennett, R. H., H. Li, P. J. Valent, J. Lipkin, and M. I. Esrig, 1984. In Situ Undrained Shear Strengths and Permeabilities Derived from Piezometer Measurements, ASTM Specialty Conference on In Situ Testing of Marine Soils, San Diego, CA (in press).

Esrig, M. I., R. C. Kirby, and R. G. Bea, Initial Development of a General Effective Stress Method for the Prediction of Axial Capacity for Driven Piles in Clay, 9th An'l. OTC, Houston, TX. May 2-5, 1977, OTC 2943, pp. 495-501.

Hollister, C. D., D. R. Anderson, and G. R. Heath, 1981. Subseabed Disposal of Nuclear Wastes, Science, V. 213, pp 1321-1326.

Levadoux, J. N. and M. M. Baligh, 1980. Pore Pressures During Cone Penetration, MIT Sea Grant report No. 80-12, 310 pp.

Miller, J. B., V. W. Miller and L. O. Olson, 1982. ISHTE Simulation: APL-UW Engineering Report, Sandia National Laboratories Contracts 74-1121 and 16-3128, Applied Physics Laboratory, University of Washington, Seattle, WA., 80 p.

Mitchell, J. K., 1976. Temperature-Volume Relationships, in Fundamentals of Soil Behavior, John Wiley Series in Soil Engineering, John Wiley and Sons, New York, N.Y., pp 274-281.

Percival, C. M., 1983. The Subseabed Disposal Program In Situ Heat Transfer Experiment (ISHTE), Sandia Report SAND80-0202, Sandia National Laboratories, Albuquerque, NM, 47 p.

Randolph, M. F., J. P. Carter, and C. P. Wroth, Driven Piles in Clay - the effects of installation and subsequent consolidation, Geotechnique, Vol. 29, No. 4, pp 495-393.

Scott, R. F., 1963. Transient Flow: Mathematical Analysis, Principles of Soil Mechanics, Addison-Wesley Publishing Company, Reading, Mass, pp. 188-206.

Shephard, L. E., 1984. Letter from Shephard, Sandia National Laboratories, Albuquerque to P. J. Valent, NORDA, dated 15 May 1984.

Silva, A. J., S. A. Jordan, and S. J. Criscenzo, 1983. Report of Simulation Experiment for In Situ Heat Transfer Experiment Project, Sandia National Laboratories Subseabed Disposal Program, University of Rhode Island, Kingston, RI, 51 p.

Silva, A. J., S. A. Jordan, and W. P. Levy, 1982. Geotechnical Studies for Subseabed Disposal of High Level Radioactive Wastes, Annual Progress Report No. 9, Departments of Ocean and Civil Engineering, University of Rhode Island, Kingston, RI, 138 p.

Soderberg, L. O., 1962. Consolidation Theory Applied to Foundation Pile Time Effects, Geotechnique, V. 12, 1962, pp 217-225.

Torstensson, B. A., 1977. The Pore Pressure Probe, Nordiske Mote, Bergmekanikk, Paper Nol 34, Oslo, Norway, pp 1-15.

Tumay, M. T. and Acar, Y. B. Piezocone Penetration Testing in Soft Cohesive Soils, ASTM Specialty Conference on In Situ Testing of Marine Soils, San Diego, CA, (in press), 16 p.

ADDENDUM I. Unadjusted Data, ISIMU-II Experiment

DATA SET 1: INSTALLATION OF PIEZOMETER 3, DATA APPEARS IN COLUMN 7

			Thermistors							P-3	P-2
Hours	Min	Sec	0	1	2	3	4	5	6		
11	52	10	23.9	23.2	23.2	23.2	23.3	24.3	23.0	-0.2534	-0.0078
11	52	20	23.9	23.2	23.2	23.2	23.2	24.3	23.0	-0.2188	-0.0078
11	52	30	23.9	23.2	23.2	23.2	23.3	24.2	23.0	0.1104	-0.0078
11	52	40	23.8	23.2	23.2	23.2	23.2	24.3	23.0	0.2129	-0.0078
11	52	50	23.8	23.2	23.1	23.2	23.3	24.3	23.0	0.2530	-0.0078
11	53	00	23.8	23.2	23.2	23.2	23.2	24.3	23.0	0.2666	-0.0078
11	53	10	23.8	23.2	23.2	23.2	23.2	24.3	23.0	0.2682	-0.0078
11	53	20	23.8	23.2	23.2	23.2	23.3	24.3	23.0	0.2638	-0.0078
11	53	30	23.9	23.2	23.2	23.2	23.3	24.3	23.0	0.2569	-0.0078
11	53	40	23.9	23.2	23.2	23.2	23.3	24.3	23.0	0.2488	-0.0078
11	53	50	23.8	23.3	23.2	23.2	23.2	24.3	23.0	0.2402	-0.0078
11	54	00	23.9	23.2	23.2	23.2	23.3	24.3	23.0	0.2316	-0.0078
11	54	10	23.9	23.2	23.2	23.2	23.3	24.3	23.0	0.2233	-0.0078
11	54	20	23.9	23.2	23.2	23.2	23.3	24.3	22.9	0.2153	-0.0078
11	54	30	23.9	23.2	23.2	23.2	23.3	24.3	23.0	0.2075	-0.0078
11	54	40	23.9	23.2	23.2	23.2	23.3	24.3	23.0	0.2003	-0.0078
11	54	50	23.9	23.2	23.1	23.2	23.3	24.3	23.0	0.1934	-0.0078
11	55	00	23.9	23.2	23.2	23.2	23.3	24.3	23.0	0.1868	-0.0078
11	55	10	23.9	23.2	23.1	23.2	23.3	24.3	23.0	0.1805	-0.0078
11	55	20	23.9	23.2	23.2	23.2	23.3	24.3	23.1	0.1745	-0.0078
11	55	30	23.9	23.2	23.2	23.2	23.3	24.3	23.0	0.1689	-0.0078
11	55	40	23.9	23.2	23.2	23.2	23.3	24.3	23.0	0.1636	-0.0079
11	55	50	23.9	23.2	23.2	23.2	23.3	24.2	23.0	0.1584	-0.0079
11	56	00	23.8	23.3	23.2	23.2	23.3	24.3	23.0	0.1536	-0.0079
11	56	10	23.9	23.2	23.2	23.2	23.3	24.2	23.0	0.1489	-0.0079
11	56	20	23.9	23.2	23.2	23.2	23.3	24.3	23.0	0.1445	-0.0079
11	56	30	23.9	23.2	23.2	23.2	23.3	24.2	23.0	0.1403	-0.0079
11	56	40	23.9	23.2	23.2	23.2	23.3	24.2	23.0	0.1362	-0.0079
11	56	50	23.9	23.2	23.2	23.2	23.2	24.2	23.0	0.1322	-0.0079
11	57	00	23.8	23.3	23.2	23.2	23.3	24.3	23.0	0.1285	-0.0079
11	57	10	23.9	23.3	23.2	23.2	23.3	24.3	23.0	0.1249	-0.0079
11	57	20	23.9	23.3	23.2	23.1	23.3	24.3	23.0	0.1215	-0.0079
11	57	30	23.9	23.2	23.2	23.2	23.3	24.3	23.0	0.1181	-0.0078
11	57	40	23.9	23.2	23.2	23.2	23.3	24.3	23.0	0.1150	-0.0079
11	57	50	23.9	23.2	23.2	23.1	23.3	24.3	23.0	0.1118	-0.0079
11	58	00	23.9	23.2	23.2	23.2	23.3	24.3	23.0	0.1088	-0.0079
11	58	10	23.9	23.3	23.2	23.2	23.2	24.3	23.0	0.1059	-0.0079
11	58	20	23.9	23.2	23.2	23.2	23.3	24.3	23.0	0.1030	-0.0079
11	58	30	24.0	23.3	23.2	23.1	23.3	24.3	23.0	0.1002	-0.0079
11	58	40	24.0	23.2	23.2	23.1	23.3	24.3	23.0	0.0976	-0.0079
11	58	50	24.0	23.2	23.2	23.2	23.3	24.3	23.0	0.0951	-0.0079
11	59	00	23.9	23.2	23.2	23.2	23.3	24.2	23.0	0.0925	-0.0080
11	59	10	24.0	23.2	23.2	23.2	23.3	24.3	23.0	0.0902	-0.0079
11	59	20	23.9	23.2	23.2	23.2	23.3	24.3	22.9	0.0879	-0.0079
11	59	30	23.9	23.3	23.2	23.2	23.3	24.3	23.0	0.0855	-0.0080
11	59	40	23.9	23.2	23.2	23.2	23.3	24.3	23.0	0.0833	-0.0080
12	01	00	23.9	23.2	23.2	23.1	23.3	24.3	23.0	0.0675	-0.0080
12	06	00	23.9	23.3	23.3	23.2	23.4	24.3	23.1	0.0265	-0.0081
12	11	00	23.8	23.3	23.2	23.2	23.3	24.2	23.1	0.0003	-0.0082
12	16	00	23.4	23.3	23.3	23.2	23.4	24.0	23.2	-0.0188	-0.0081

			Thermistors								
Hours	Min	Sec	0	1	2	3	4	5	6	P-3	P-2
12	21	00	23.2	23.2	23.2	23.2	23.3	23.7	23.0	-0.0337	-0.0080
12	26	00	22.9	23.2	23.2	23.1	23.3	23.5	23.0	-0.0456	-0.0079
12	31	00	23.0	23.2	23.1	23.1	23.2	23.6	22.9	-0.0555	-0.0079
12	36	00	23.3	23.2	23.1	23.1	23.3	24.0	23.0	-0.0638	-0.0080
12	41	00	23.6	23.2	23.2	23.2	23.2	24.2	23.0	-0.0712	-0.0081
12	46	00	23.9	23.3	23.2	23.2	23.3	24.1	23.0	-0.0775	-0.0083
12	51	00	24.0	23.3	23.3	23.3	23.3	24.2	23.0	-0.0832	-0.0097
12	56	00	24.1	23.3	23.3	23.3	23.4	24.2	23.0	-0.0885	-0.0095
13	01	00	24.1	23.3	23.3	23.3	23.4	24.2	23.0	-0.0928	-0.0095
13	06	00	24.2	23.5	23.4	23.4	23.5	24.4	23.0	-0.0967	-0.0095
13	11	00	24.1	23.5	23.5	23.5	23.5	24.4	23.0	-0.1003	-0.0069
13	16	00	23.8	23.5	23.4	23.4	23.5	24.0	23.0	-0.1037	-0.0068
13	21	00	23.6	23.4	23.4	23.4	23.5	23.8	23.1	-0.1062	-0.0066
13	26	00	23.4	23.4	23.3	23.3	23.5	23.7	23.0	-0.1086	-0.0066
13	31	00	23.1	23.4	23.3	23.3	23.4	23.6	23.0	-0.1107	-0.0065
13	36	00	23.1	23.3	23.2	23.2	23.4	23.5	23.0	-0.1126	-0.0064
13	41	00	23.0	23.3	23.3	23.2	23.4	23.5	23.0	-0.1142	-0.0063
13	46	00	22.9	23.2	23.2	23.1	23.3	23.4	22.8	-0.1156	-0.0061
13	51	00	23.2	23.2	23.2	23.1	23.3	23.6	22.9	-0.1172	-0.0061
13	56	00	23.5	23.5	23.3	23.1	23.4	23.8	23.0	-0.1184	-0.0063
14	01	00	23.5	29.9	32.7	31.4	32.7	23.9	23.0	-0.1201	-0.0064
14	06	00	23.4	30.5	30.6	29.4	30.7	23.5	23.0	-0.1213	-0.0066
14	11	00	22.9	31.6	31.0	28.9	31.0	23.6	23.0	-0.1216	-0.0068
14	16	00	23.1	30.3	29.9	28.5	30.0	23.9	23.0	-0.1104	-0.0068
14	21	00	23.0	29.6	29.2	28.2	29.2	23.9	23.1	-0.1196	-0.0069
14	23	59	23.1	29.1	28.8	27.9	28.8	24.0	23.1	-0.1217	-0.0071
14	24	20	23.1	29.1	28.7	27.9	28.8	23.9	23.1	-0.1220	-0.0070
14	24	40	23.0	29.0	28.7	27.8	28.7	24.0	23.0	-0.1223	-0.0071
14	25	00	23.0	29.0	28.6	27.9	28.8	23.9	23.1	-0.1224	-0.0070
14	25	20	23.1	29.1	28.7	27.8	28.7	23.9	23.1	-0.1226	-0.0071
14	25	40	23.1	29.1	28.6	27.8	28.7	23.9	23.2	-0.1227	-0.0071
14	26	00	23.1	28.9	28.5	27.8	28.7	23.9	23.0	-0.1228	-0.0071
14	26	20	23.1	28.8	28.7	27.8	28.7	23.9	23.0	-0.1232	-0.0071
14	26	50	23.1	25.1	26.3	27.1	26.0	23.9	23.1	-0.1232	-0.0071
14	27	30	23.0	22.9	23.9	26.1	23.3	23.7	23.0	-0.1233	-0.0070
14	28	00	23.1	22.2	23.0	24.6	22.8	23.7	23.1	-0.1236	-0.0071

Data Set 2: INSTALLATION OF HEATER.
DATA APPEARS IN COLUMN 7.

14	28	10	23.1	22.0	22.8	24.2	22.7	23.7	23.0	-0.1237	-0.0071
14	28	20	23.1	21.7	22.4	23.6	22.3	23.6	23.1	-0.0184	-0.0071
14	28	30	23.1	22.2	22.5	23.1	22.5	23.6	23.1	-0.0066	-0.0070
14	28	40	23.1	22.3	22.5	23.1	22.6	23.6	23.1	0.0111	-0.0071
14	28	50	23.1	22.4	22.6	23.1	22.7	23.6	23.1	0.0231	-0.0071
14	29	00	23.1	22.4	22.6	23.2	22.7	23.6	23.1	0.0315	-0.0071
14	29	10	23.1	22.5	22.6	23.1	22.7	23.5	23.0	0.0377	-0.0071
14	29	20	23.1	22.5	22.6	23.1	22.7	23.5	23.0	0.0419	-0.0071
14	29	30	23.1	22.5	22.7	23.1	22.7	23.5	23.1	0.0461	-0.0071
14	29	40	23.1	22.6	22.6	23.1	22.8	23.5	23.0	0.0488	-0.0070
14	29	50	23.0	22.6	22.7	23.1	22.7	23.5	23.1	0.0508	-0.0070
14	30	00	23.1	22.6	22.6	23.1	22.8	23.4	23.0	0.0525	-0.0070
14	30	10						23.4		0.0538	-0.0070

			Thermistors								
Hours	Min	Sec	0	1	2	3	4	5	6	P-3	P-2
14	30	20	23.0	22.6	22.7	23.0	22.8	23.4	23.0	0.0548	-0.0070
14	30	30	23.1	22.7	22.7	23.0	22.8	23.4	23.1	0.0557	-0.0070
14	30	40	23.0	22.7	22.7	23.0	22.8	23.5	23.1	0.0564	-0.0071
14	30	50	23.1	22.7	22.7	23.0	22.8	23.4	23.1	0.0569	-0.0070
14	31	00	23.1	22.7	22.7	23.0	22.9	23.4	23.1	0.0570	-0.0070
14	31	10	23.1	22.7	22.7	23.0	22.8	23.4	23.1	0.0573	-0.0071
14	31	20	23.1	22.7	22.7	23.0	22.8	23.3	23.1	0.0575	-0.0070
14	31	30	23.1	22.7	22.7	23.0	22.8	23.3	23.1	0.0577	-0.0070
14	31	50	23.1	22.7	22.8	23.0	22.8	23.3	23.1	0.0577	-0.0071
14	32	00	23.1	22.7	22.7	23.0	22.9	23.3	23.0	0.0575	-0.0070
14	32	10	23.0	22.7	22.8	23.0	22.8	23.3	23.1	0.0574	-0.0071
14	32	20	23.1	22.7	22.7	23.0	22.8	23.3	23.1	0.0571	-0.0071
14	32	30	23.1	22.7	22.8	23.0	22.8	23.3	23.1	0.0568	-0.0071
14	32	40	23.1	22.7	22.8	23.0	22.8	23.3	23.0	0.0567	-0.0070
14	32	50	23.1	22.7	22.8	23.0	22.9	23.3	23.1	0.0564	-0.0070
14	33	00	23.1	22.8	22.8	23.0	22.8	23.8	23.1	0.0562	-0.0070
14	33	10	23.1	22.7	22.7	23.0	22.9	23.7	23.0	0.0559	-0.0071
14	33	20	23.0	22.8	22.8	22.9	22.8	23.6	23.1	0.0556	-0.0070
14	33	30	23.0	22.8	22.8	23.0	22.9	23.5	23.1	0.0552	-0.0071
14	33	40	23.0	22.8	22.8	22.9	22.8	23.5	23.1	0.0549	-0.0070
14	33	50	23.1	22.8	22.8	23.0	22.9	23.5	23.1	0.0544	-0.0071
14	34	00	23.1	22.8	22.8	22.9	22.9	23.5	23.1	0.0541	-0.0070
14	34	10	23.1	22.8	22.8	23.0	22.9	23.4	23.1	0.0535	-0.0071
14	34	20	23.1	22.8	22.8	22.9	22.9	23.4	23.0	0.0532	-0.0070
14	34	30	23.0	22.8	22.8	22.9	22.9	23.4	23.1	0.0529	-0.0070
14	34	40	23.1	22.8	22.8	22.9	22.9	23.3	23.1	0.0524	-0.0070
14	34	50	23.1	22.9	22.9	22.9	22.9	23.3	23.2	0.0521	-0.0070
14	35	00	23.1	22.8	22.8	22.9	22.9	23.3	23.0	0.0516	-0.0070
14	35	10	23.1	22.8	22.8	22.9	22.9	23.3	23.1	0.0512	-0.0070
14	35	20	23.1	22.8	22.8	22.9	22.9	23.3	23.1	0.0508	-0.0070
14	35	30	23.1	22.7	22.8	22.9	22.8	23.2	23.1	0.0506	-0.0070
14	35	40	23.1	22.7	22.9	22.9	22.9	23.3	23.0	0.0503	-0.0070
14	35	50	23.1	22.9	22.8	23.0	22.9	23.2	23.1	0.0497	-0.0070
14	36	00	23.0	22.9	22.8	22.9	22.8	23.2	23.0	0.0492	-0.0070
14	36	10	23.1	22.8	22.8	22.9	22.9	23.2	23.0	0.0488	-0.0070
14	36	20	23.1	22.8	22.8	22.9	22.9	23.2	23.1	0.0483	-0.0069
14	36	30	23.1	22.9	22.9	22.9	22.9	23.2	23.1	0.0478	-0.0070
14	36	40	23.1	22.8	22.8	22.9	22.9	23.1	23.1	0.0475	-0.0070
14	36	50	23.1	22.9	22.8	22.9	22.9	23.1	23.1	0.0471	-0.0069
14	37	00	23.1	22.8	22.8	22.9	22.9	23.1	23.1	0.0465	-0.0070
14	37	10	23.1	22.8	22.8	22.9	22.9	23.1	23.1	0.0462	-0.0069
14	37	20	23.1	22.8	22.9	22.9	22.9	23.1	23.1	0.0459	-0.0069
14	37	30	23.1	22.8	22.8	22.9	22.9	23.1	23.0	0.0454	-0.0069
14	37	40	23.1	22.9	22.8	22.9	22.9	23.0	23.0	0.0448	-0.0069
14	37	50	23.1	22.8	22.8	22.9	22.9	23.0	23.0	0.0445	-0.0069
14	38	00	23.1	22.8	22.9	22.9	22.9	23.0	23.1	0.0440	-0.0069
14	38	10	23.1	22.7	22.8	22.9	22.9	23.1	23.0	0.0436	-0.0069
14	38	20	23.1	22.7	22.8	22.9	22.9	23.1	23.0	0.0431	-0.0069
14	38	30	23.1	22.8	22.8	22.9	22.9	23.0	23.0	0.0427	-0.0069
14	38	40	23.0	22.8	22.9	22.9	22.9	23.0	23.2	0.0422	-0.0069
14	38	50	23.1	22.8	22.8	22.9	22.9	23.0	23.0	0.0418	-0.0069
14	39	00	23.0	22.8	22.9	22.9	22.9	23.0	23.0	0.0414	-0.0068
14	39	10	23.1	22.8	22.8	22.9	22.9	23.0	23.1	0.0409	-0.0068
14	39	20	23.1	22.8	22.8	22.9	22.9	23.0	23.0	0.0404	-0.0069

			Thermistors								
Hours	Min	Sec	0	1	2	3	4	5	6	P-3	P-2
14	39	30	23.1	22.8	22.8	22.9	22.9	23.0	23.1	0.0400	-0.0069
14	39	40	23.1	22.8	22.8	22.9	22.9	23.0	23.1	0.0394	-0.0069
14	39	50	23.1	22.8	22.8	22.9	22.9	23.0	23.1	0.0389	-0.0068
14	40	05	23.1	22.8	22.8	22.9	22.9	23 0	23.1	0.0383	-0.0068
14	41	00	23.1	22.8	22.9	22.9	22.9	22.9	23.1	0.0359	-0.0069
14	46	00	23.1	22.8	22.8	22.9	22.9	22.8	23.1	0.0234	-0.0068
14	51	00	23.0	22.9	22.9	22.9	22.9	22.6	23.1	0.0123	-0.0066
14	56	00	23.1	22.8	22.8	22.9	22.9	22.5	23.0	0.0025	-0.0065
15	01	00	23.0	22.8	22.8	22.8	22.9	22.4	23.0	-0.0063	-0.0063
15	06	00	23.0	22.9	22.8	22.9	23.0	22.4	23.0	-0.0140	-0.0061
15	11	00	22.9	22.8	22.8	22.8	22.9	22.2	23.0	-0.0214	-0.0060
15	16	00	23.0	22.8	22.9	22.8	22.9	22.3	23.0	-0.0278	-0.0058
15	21	00	23.0	22.9	22.9	22.8	23.0	22.4	23.0	-0.0339	-0.0058
15	26	00	23.0	22.9	22.9	22.8	23.0	22.8	23.0	-0.0393	-0.0058
15	31	00	23.0	22.9	22.9	22.8	23.0	22.9	23.0	-0.0444	-0.0060
15	36	00	23.0	22.8	22.9	22.8	23.0	22.8	23.0	-0.0491	-0.0061
15	41	00	23.0	22.8	22.8	22.8	23.0	22.9	23.0	-0.0536	-0.0063
15	46	00	23.0	22.8	22.9	22.8	22.9	23.2	23.1	-0.0577	-0.0064
15	51	00	22.9	22.9	22.8	22.8	22.9	23.1	22.8	-0.0619	-0.0066
15	56	00	22.9	22.8	22.8	22.8	22.9	22.9	23.0	-0.0654	-0.0066
16	01	00	22.9	22.8	22.8	22.8	22.9	23.0	23.0	-0.0689	-0.0066
16	06	00	23.0	22.8	22.8	22.8	22.9	23.2	23.0	-0.0722	-0.0068
16	11	00	23.0	22.8	22.8	22.8	22.9	22.8	23.0	-0.0752	-0.0068
16	16	00	22.9	22.8	22.8	22.8	22.9	22.6	23.0	-0.0782	-0.0067
16	18	42	22.9	22.9	22.8	22.8	22.9	22.6	23.0	-0.0795	-0.0067
16	18	56	23.0	22.9	22.8	22.8	22.9	22.6	23.0	-0.0798	-0.0066
16	24	09	23.0	22.8	22.9	22.8	22.9	22.5	23.0	-0.0822	-0.0066
16	30	00	23.0	22.9	22.8	22.8	22.9	22.4	23.0	-0.0850	-0.0064
16	40	00	23.0	22.9	22.9	22.8	23.0	22.2	23.0	-0.0890	-0.0062
16	50	00	23.0	22.8	22.8	22.8	23.0	22.4	23.0	-0.0926	-0.0062
17	00	00	23.0	22.8	22.8	22.8	22.9	23.1	23.0	-0.0963	-0.0064
17	10	00	23.0	22.8	22.8	22.8	22.9	23.4	23.0	-0.1001	-0.0068
17	20	00	23.0	22.8	22.8	22.8	22.9	23.4	23.0	-0.1038	-0.0069
17	30	00	23.0	22.8	22.9	22.8	22.9	23.5	23.1	-0.1072	-0.0071
17	40	00	23.1	22.8	22.9	22.8	22.9	23.6	23.1	-0.1102	-0.0073
17	50	00	23.0	22.8	22.8	22.8	22.9	23.6	23.0	-0.1132	-0.0074
18	00	00	23.1	22.8	22.8	22.8	22.9	23.7	23.1	-0.1159	-0.0075
18	10	00	23.1	22.8	22.8	22.8	23.0	23.7	23.1	-0.1183	-0.0076
18	20	00	23.1	22.8	22.8	22.8	22.9	23.8	23.1	-0.1205	-0.0076
18	30	00	23.1	22.8	22.8	22.8	22.9	23.8	23.1	-0.1227	-0.0077
18	40	00	23.0	22.7	22.8	22.8	22.9	23.7	23.1	-0.1247	-0.0077
18	50	00	23.1	22.7	22.8	22.7	22.9	23.8	23.1	-0.1264	-0.0078
19	00	00	23.1	22.8	22.8	22.8	22.9	23.9	23.2	-0.1281	-0.0079
19	10	00	23.2	22.8	22.8	22.8	23.0	23.9	23.2	-0.1298	-0.0078
19	20	00	23.2	22.9	22.9	22.8	22.9	23.9	23.2	-0.1312	-0.0079
19	30	00	23.2	22.9	22.9	22.8	22.9	24.0	23.3	-0.1324	-0.0079
19	40	00	23.2	22.9	22.8	22.8	22.9	24.0	23.2	-0.1336	-0.0079
19	50	00	23.2	22.8	22.9	22.8	22.9	23.9	23.2	-0.1346	-0.0078
20	00	00	23.2	22.8	22.8	22.8	22.9	23.8	23.2	-0.1356	-0.0078
20	10	00	23.1	22.8	22.8	22.8	22.9	23.9	23.2	-0.1366	-0.0078
20	20	00	23.1	22.8	22.8	22.8	22.9	23.9	23.2	-0.1376	-0.0078
20	30	00	23.2	22.9	22.8	22.8	22.9	24.0	23.3	-0.1385	-0.0079
20	40	00	23.2	22.9	22.8	22.8	22.9	24.0	23.3	-0.1394	-0.0079
20	50	00	23.2	22.9	22.8	22.8	22.9	23.9	23.3	-0.1402	-0.0079

			Thermistors								
Hours	Min	Sec	0	1	2	3	4	5	6	P-3	P-2
21	00	00	23.2	22.9	22.8	22.8	22.9	23.9	23.3	-0.1408	-0.0078
21	10	00	23.2	22.9	22.8	22.8	22.9	23.9	23.3	-0.1415	-0.0075
21	20	00	23.3	22.9	22.9	22.8	23.0	23.9	23.3	-0.1421	-0.0078
21	30	00	23.2	22.8	22.8	22.8	22.9	23.8	23.3	-0.1424	-0.0075
21	40	00	23.2	22.9	22.8	22.8	22.9	23.8	23.3	-0.1428	-0.0078
21	50	00	23.2	22.9	22.8	22.8	22.9	23.9	23.3	-0.1431	-0.0077
22	00	00	23.2	22.8	22.8	22.8	22.9	23.8	23.3	-0.1435	-0.0077
22	10	00	23.3	22.9	22.8	22.8	23.0	24.0	23.3	-0.1441	-0.0077
22	20	00	23.2	22.9	22.8	22.8	22.9	24.0	23.3	-0.1445	-0.0077
22	30	00	23.2	22.9	22.8	22.8	22.9	23.9	23.3	-0.1450	-0.0078
22	40	00	23.3	22.9	22.9	22.9	23.0	24.0	23.4	-0.1454	-0.0078
22	50	00	23.3	22.9	22.9	22.8	22.9	24.0	23.4	-0.1458	-0.0078
23	00	00	23.3	22.9	22.9	22.8	23.0	23.9	23.4	-0.1460	-0.0078
23	10	00	23.3	22.9	22.9	22.8	23.0	23.9	23.4	-0.1461	-0.0077
23	20	00	23.3	22.9	22.9	22.9	22.9	23.9	23.4	-0.1464	-0.0077
23	30	00	23.3	22.9	22.8	22.8	22.9	23.8	23.4	-0.1466	-0.0076
23	40	00	23.2	22.9	22.8	22.8	22.9	23.8	23.4	-0.1468	-0.0076
23	50	00	23.3	23.0	22.9	22.8	23.0	23.8	23.4	-0.1470	-0.0076
24	20	00	23.3	22.0	22.8	22.9	23.0	23.7	23.4	-0.1470	-0.0075
24	50	00	23.3	22.9	22.8	22.8	22.9	23.5	23.3	-0.1469	-0.0075
25	20	00	23.2	23.0	22.9	22.8	22.9	23.5	23.4	-0.1468	-0.0074
25	50	00	23.2	23.0	22.9	22.9	23.0	23.4	23.4	-0.1466	-0.0074
26	20	00	23.2	23.0	22.9	22.9	23.0	23.3	23.4	-0.1464	-0.0073
26	50	00	23.3	23.1	23.0	22.9	23.1	23.3	23.4	-0.1462	-0.0072
27	20	00	23.2	23.0	22.9	22.9	23.0	23.2	23.3	-0.1459	-0.0072
27	50	00	23.2	23.0	23.0	22.9	23.0	22.9	23.3	-0.1456	-0.0071
28	20	00	23.2	23.1	23.0	23.0	23.1	22.9	23.4	-0.1451	-0.0070
28	50	00	23.1	23.1	23.0	23.0	23.1	22.9	23.3	-0.1447	-0.0071
29	20	00	23.1	23.1	23.0	23.0	23.1	22.7	23.3	-0.1444	-0.0070
29	50	00	23.1	23.1	23.0	23.0	23.1	22.7	23.3	-0.1441	-0.0069
30	20	00	23.1	23.1	23.0	23.0	23.1	22.9	23.2	-0.1436	-0.0070
30	40	00	22.9	23.1	23.0	22.0	23.1	19.7	23.1	-0.1415	-0.0049
30	50	00	22.9	23.1	23.0	23.0	23.1	22.0	23.0	-0.1395	-0.0050
31	00	00	22.9	23.1	23.0	23.0	23.2	22.6	23.0	-0.1390	-0.0055
31	30	00	22.9	23.1	23.0	23.0	23.1	23.0	23.0	-0.1389	-0.0053
32	00	00	23.0	23.2	23.1	23.0	23.2	23.1	23.1	-0.1394	-0.0063
32	20	00	23.0	23.1	23.1	23.0	23.1	22.8	23.0	-0.1385	-0.0001

DATA SET 3: INSTALLATION OF SECOND PIEZOMETER. DATA FROM 2nd (P-2) APPEARS IN COL. 8. DATA FROM 1st (P-3) APPEARS IN COL. 7.

09	24	20	23.0	22.9	23.0	23.0	23.1	23.5	23.0	-0.1405	-0.2259
09	24	30	23.0	23.0	23.0	22.9	23.0	23.5	23.0	-0.1390	-0.1737
09	24	40	23.0	23.1	23.0	23.0	23.1	23.5	23.0	-0.1291	0.2112
09	24	50	23.0	23.1	23.1	23.0	23.1	23.5	23.1	-0.1237	0.2403
09	25	00	23.0	23.1	23.0	23.0	23.1	23.5	23.1	-0.1196	0.2441
09	25	10	23.0	23.2	23.0	23.0	23.2	23.5	23.1	-0.1166	0.2424
09	25	20	23.0	23.1	23.1	23.0	23.1	23.5	23.1	-0.1142	0.2385
09	25	30	23.0	23.1	23.0	23.0	23.1	23.5	23.1	-0.1124	0.2336
09	25	40	23.1	23.2	23.1	23.0	23.2	23.5	23.2	-0.1110	0.2283
09	25	50	23.0	23.1	23.0	23.0	23.1	23.5	23.1	-0.1098	0.2230
09	26	00	23.0	23.1	23.0	23.0	23.1	23.5	23.1	-0.1088	0.2177
09	26	10	23.0	23.1	23.0	23.0	23.1	23.5	23.1	-0.1082	0.2124

			Thermistors								
Hours	Min	Sec	0	1	2	3	4	5	6	P-3	P-2
09	26	20	23.0	23.1	23.0	23.0	23.1	23.5	23.1	-0.1076	0.2074
09	26	30	23.0	23.1	23.0	23.0	23.1	23.4	23.1	-0.1071	0.202e
09	26	40	23.1	23.2	23.0	23.1	23.2	23.5	23.1	-0.1067	0.1979
09	26	50	23.1	23.2	23.0	23.0	23.2	23.5	23.1	-0.1065	0.1934
09	27	00	23.0	23.2	23.1	23.0	23.2	23.5	23.1	-0.1062	0.1891
09	27	10	23.0	23.1	23.0	23.0	23.1	23.5	23.1	-0.1061	0.1849
09	27	20	23.1	23.2	23.1	23.0	23.1	23.5	23.1	-0.1060	0.1810
09	27	30	23.1	23.1	23.1	23.0	23.1	23.5	23.1	-0.1059	0.1771
09	27	40	23.1	23.1	23.0	23.1	23.2	23.5	23.1	-0.1058	0.1735
09	27	50	23.1	23.2	23.1	23.0	23.2	23.5	23.1	-0.1058	0.1699
09	28	00	23.1	23.2	23.1	23.0	23.2	23.5	23.1	-0.1058	0.1661
09	28	10	23.0	23.1	23.1	23.0	23.1	23.5	23.2	-0.1057	0.1627
09	28	20	23.0	23.1	23.1	23.0	23.1	23.5	23.1	-0.1057	0.1594
09	28	30	23.0	23.1	23.1	23.1	23.1	23.5	23.1	-0.1057	0.1564
09	28	40	23.1	23.2	23.1	23.0	23.1	23.5	23.1	-0.1057	0.1534
09	28	50	23.0	23.1	23.1	23.0	23.2	23.5	23.1	-0.1058	0.150e
09	29	00	23.0	23.1	23.1	23.0	23.1	23.5	23.1	-0.1058	0.1478
09	29	10	23.0	23.1	23.1	23.1	23.1	23.5	23.1	-0.1059	0.1450
09	29	20	23.0	23.2	23.1	23.0	23.1	23.5	23.1	-0.1059	0.1424
09	29	30	23.1	23.1	23.1	23.0	23.2	23.5	23.1	-0.1059	0.1399
09	29	40	23.0	23.1	23.0	23.0	23.2	23.5	23.1	-0.1059	0.1374
09	29	50	23.0	23.1	23.1	23.0	23.2	23.5	23.1	-0.1060	0.1349
09	30	00	23.0	23.2	23.1	23.0	23.1	23.5	23.1	-0.1060	0.1327
09	30	10	23.1	23.2	23.1	23.1	23.2	23.5	23.2	-0.1061	0.1304
09	30	20	23.1	23.1	23.1	23.0	23.1	23.5	23.1	-0.1061	0.1282
09	30	30	23.0	23.1	23.1	23.0	23.2	23.6	23.1	-0.1061	0.1261
09	30	40	23.0	23.2	23.0	23.0	23.2	23.5	23.1	-0.1062	0.1239
09	30	50	23.1	23.1	23.0	23.0	23.2	23.5	23.1	-0.1063	0.1219
09	31	00	23.0	23.1	23.0	23.0	23.1	23.5	23.1	-0.1062	0.1199
09	31	10	23.0	23.1	23.1	23.0	23.1	23.5	23.1	-0.1063	0.1180
09	31	20	23.1	23.1	23.0	23.0	23.2	23.4	23.1	-0.1064	0.116e
09	31	30	23.1	23.2	23.1	23.1	23.2	23.5	23.1	-0.1064	0.1141
09	31	40	23.1	23.2	23.1	23.1	23.2	23.5	23.1	-0.1064	0.1123
09	31	50	23.1	23.2	23.1	23.0	23.1	23.4	23.2	-0.1064	0.1105
09	32	00	23.0	23.1	23.0	23.0	23.1	23.4	23.1	-0.1064	0.1087
09	32	10	23.1	23.2	23.1	23.0	23.1	23.4	23.1	-0.1065	0.1071
09	32	20	23.1	23.2	23.1	23.0	23.1	23.4	23.1	-0.1065	0.1054
09	32	30	23.1	23.2	23.1	23.0	23.2	23.4	23.1	-0.1066	0.1038
09	32	40	23.1	23.2	23.0	23.1	23.2	23.3	23.1	-0.1066	0.1021
09	32	50	23.1	23.2	23.0	23.0	23.2	23.3	23.1	-0.1066	0.1005
09	33	00	23.1	23.2	23.1	23.0	23.1	23.3	23.1	-0.1066	0.0990
09	33	10	23.1	23.2	23.1	23.0	23.1	23.2	23.1	-0.1066	0.0975
09	33	20	23.1	23.2	23.1	23.0	23.1	23.2	23.1	-0.1067	0.0959
09	33	30	23.1	23.2	23.1	23.0	23.1	23.2	23.1	-0.1067	0.0944
09	33	40	23.1	23.2	23.1	23.0	23.2	23.1	23.1	-0.1067	0.0930
09	33	50	23.0	23.2	23.1	23.0	23.1	23.1	23.1	-0.1067	0.0917
09	34	00	23.1	23.2	23.0	23.0	23.2	23.1	23.1	-0.1068	0.0903
09	34	10	23.1	23.2	23.1	23.0	23.2	23.0	23.1	-0.1068	0.0889
09	34	20	23.1	23.1	23.0	23.0	23.1	23.0	23.1	-0.1068	0.087e
09	34	30	23.0	23.1	23.1	23.0	23.1	22.9	23.1	-0.1069	0.0861
09	34	40	23.0	23.1	23.1	23.0	23.1	22.9	23.1	-0.1069	0.0848
09	34	50	23.1	23.2	23.1	23.0	23.2	23.0	23.2	-0.1069	0.0835
09	35	00	23.1	23.1	23.1	23.0	23.1	22.8	23.1	-0.1069	0.0823
09	35	10	23.0	23.1	23.1	23.0	23.1	22.8	23.1	-0.1069	0.0810

			Thermistors								
Hours	Min	Sec	0	1	2	3	4	5	6	P-3	P-2
09	35	20	23.1	23.2	23.1	23.0	23.1	22.8	23.1	-0.1069	0.0798
09	35	30	23.1	23.2	23.1	23.0	23.2	22.8	23.1	-0.1070	0.0785
09	35	40	23.1	23.1	23.0	23.0	23.2	22.7	23.1	-0.1070	0.0774
09	35	50	23.1	23.2	23.1	23.1	23.2	22.8	23.1	-0.1070	0.0762
09	36	00	23.1	23.1	23.0	23.0	23.1	22.7	23.1	-0.1070	0.0751
09	36	10	23.1	23.2	23.1	23.0	23.2	22.7	23.2	-0.1071	0.0740
09	40	00	23.1	23.2	23.0	23.0	23.1	22.2	23.1	-0.1074	0.0513
09	45	00	23.0	23.1	23.0	23.0	23.1	22.3	23.1	-0.1078	0.0290
09	50	00	23.0	23.1	23.0	22.9	23.1	23.0	23.1	-0.1086	0.0113
09	55	00	23.1	23.1	23.0	23.0	23.1	23.2	23.1	-0.1096	-0.0031
10	00	00	23.0	23.1	23.0	23.0	23.1	23.3	23.1	-0.1109	-0.0151
10	05	00	23.1	23.1	23.0	23.0	23.2	23.4	23.1	-0.1121	-0.0250
10	10	00	23.1	23.2	23.0	23.0	23.2	23.4	23.1	-0.1135	-0.0358
10	15	00	23.0	23.1	23.1	23.0	23.1	23.5	23.1	-0.1149	-0.0411
10	20	00	23.0	23.1	23.0	23.0	23.1	23.1	23.1	-0.1161	-0.0474
10	25	00	23.0	23.1	23.0	23.0	23.1	22.4	23.1	-0.1173	-0.0532
10	30	00	23.0	23.1	23.0	23.0	23.1	22.1	23.1	-0.1185	-0.0584
10	35	00	23.0	23.1	23.0	23.0	23.2	22.5	23.1	-0.1192	-0.0630
10	40	00	23.0	23.1	23.0	23.0	23.1	22.9	23.1	-0.1203	-0.0671
10	45	00	23.0	23.2	23.1	23.0	23.2	23.2	23.1	-0.1213	-0.0708
10	50	00	23.1	23.2	23.1	23.1	23.2	23.3	23.1	-0.1223	-0.0741
10	55	00	23.0	23.1	23.1	23.0	23.1	23.4	23.1	-0.1234	-0.0771
11	00	00	23.0	23.1	23.1	23.0	23.1	23.4	23.1	-0.1244	-0.0797
11	05	00	23.0	23.1	22.9	22.9	23.1	23.5	23.3	-0.1253	-0.0819
11	10	00	23.1	23.1	23.1	23.0	23.1	23.7	23.1	-0.1263	-0.0845
11	15	00	23.1	23.1	23.1	23.0	23.1	23.1	23.1	-0.1272	-0.0866
11	20	00	23.0	23.1	23.0	23.0	23.1	22.7	23.1	-0.1280	-0.0886
11	20	30	23.1	23.2	23.1	23.0	23.1	22.7	23.2	-0.1281	-0.0887
11	21	30	23.0	23.1	23.0	23.0	23.1	22.5	23.1	-0.1283	-0.0890
11	22	30	23.1	23.2	23.0	23.0	23.1	22.6	23.1	-0.1284	-0.0894
DATA SET 4: HEATER PROBE TURNED ON											
11	23	00	23.3	23.3	22.7	22.8	23.4	22.7	23.0	-0.1285	-0.0893
11	23	30	23.4	24.4	24.8	25.1	25.2	22.4	22.8	-0.1284	-0.0897
11	24	00	23.1	25.6	27.2	27.2	27.0	22.2	23.0	-0.1288	-0.0898
11	24	30	23.4	27.2	29.0	28.5	29.0	22.8	23.0	-0.1296	-0.0903
11	25	00	23.2	27.5	30.1	29.7	30.1	22.1	22.8	-0.1291	-0.0906
11	25	30	23.3	28.9	31.5	30.7	31.5	22.5	22.9	-0.1299	-0.0909
11	26	00	23.3	29.7	32.6	31.3	32.6	22.7	22.9	-0.1296	-0.0910
11	27	00	23.5	30.8	34.5	33.4	34.8	22.3	22.8	-0.1290	-0.0914
11	28	00	23.5	32.0	36.2	34.9	36.4	22.3	22.8	-0.1282	-0.0913
11	29	00	23.1	32.8	37.8	36.1	37.5	22.0	23.0	-0.1273	-0.0908
11	30	00	23.2	33.7	38.9	37.2	38.7	22.0	22.9	-0.1262	-0.0907
11	31	00	22.8	34.6	40.6	38.1	39.5	22.2	23.3	-0.1253	-0.0905
11	32	00	22.8	35.4	41.6	39.0	40.6	22.2	23.1	-0.1241	-0.0900
11	33	00	23.2	36.3	42.1	39.5	42.0	22.4	22.9	-0.1234	-0.0891
11	34	00	23.0	36.5	43.1	40.7	42.6	22.0	23.1	-0.1222	-0.0887
11	35	00	22.7	37.4	44.0	41.0	43.0	22.4	23.3	-0.1209	-0.0883
11	36	00	22.6	38.0	44.9	41.5	43.6	22.6	23.3	-0.1203	-0.0877
11	37	00	23.3	38.9	45.1	42.2	45.1	22.9	22.9	-0.1194	-0.0870
11	39	00	22.7	39.5	46.8	43.4	45.8	23.0	23.3	-0.1175	-0.0863
11	41	00	22.8	40.2	47.9	44.6	47.0	22.9	23.2	-0.1163	-0.0854
11	43	00	22.8	41.3	48.9	45.2	47.9	23.3	23.2	-0.1147	-0.0845

			Thermistors								
Hours	Min	Sec	0	1	2	3	4	5	6	P-3	P-2
11	45	00	22.8	42.5	50.1	45.9	49.0	23.9	23.5	-0.1141	-0.0836
11	47	00	23.5	43.1	50.3	46.7	50.4	23.8	23.0	-0.1132	-0.0827
11	50	00	23.4	44.1	51.5	47.7	51.5	23.9	23.1	-0.1118	-0.0816
11	54	00	22.9	45.2	53.3	48.7	52.2	24.1	23.6	-0.1101	-0.0807
11	57	00	23.1	45.2	53.6	49.7	53.2	23.4	22.9	-0.1089	-0.0795
12	07	00	23.1	48.0	56.2	51.3	55.6	24.3	23.3	-0.1069	-0.0783
12	19	00	23.1	49.2	58.1	53.8	57.8	22.3	23.1	-0.1051	-0.0771
12	31	00	22.9	50.7	59.7	55.1	59.4	22.0	23.0	-0.1036	-0.0769
12	39	00	23.0	52.3	60.8	55.5	60.5	22.7	23.1	-0.1033	-0.0774
12	49	00	22.8	52.3	62.0	57.1	61.1	22.5	23.3	-0.1028	-0.0785
12	59	00	23.0	53.9	63.0	57.5	62.3	23.4	23.3	-0.1033	-0.0792
13	14	00	23.0	54.3	63.6	58.7	63.4	22.8	23.0	-0.1039	-0.0809
13	24	00	23.0	55.5	64.7	59.1	64.1	23.5	23.4	-0.1052	-0.0823
13	34	00	23.0	56.1	65.4	59.7	64.7	23.7	23.5	-0.1066	-0.0827
13	44	00	23.0	56.0	65.4	60.5	65.2	22.7	23.0	-0.1071	-0.0836
13	54	00	23.1	57.1	66.3	60.6	65.8	23.2	23.3	-0.1080	-0.0852
14	04	00	22.7	57.0	66.8	61.3	65.9	22.5	23.3	-0.1084	-0.0862
14	14	00	22.6	57.3	67.2	61.6	66.2	22.5	23.4	-0.1093	-0.0872
14	24	00	23.1	57.6	67.7	62.5	66.9	22.3	23.5	-0.1101	-0.0883
14	34	00	23.2	58.7	68.0	62.2	67.6	23.0	23.3	-0.1110	-0.0890
14	44	00	23.5	58.8	68.1	62.8	68.1	22.7	23.1	-0.1119	-0.0895
14	54	00	23.6	58.8	68.3	63.3	68.5	22.5	23.0	-0.1123	-0.0904
15	04	00	23.2	58.8	69.0	63.7	68.3	22.3	23.6	-0.1132	-0.0915
15	14	00	23.4	59.9	69.4	63.6	68.8	22.9	23.6	-0.1144	-0.0923
15	24	00	23.9	59.9	69.2	64.2	69.6	22.6	23.4	-0.1148	-0.0927
15	34	00	23.4	60.4	69.8	63.9	69.4	23.2	23.5	-0.1158	-0.0935
07	10	00	23.8	24.3	24.3	24.3	24.4	20.8	23.9	-0.1460	-0.1197
07	20	00	23.8	24.4	24.3	24.3	24.5	21.0	23.9	-0.1440	-0.1198
07	30	00	23.7	24.3	24.3	24.2	24.4	21.2	23.8	-0.1424	-0.1196
07	40	00	23.6	24.3	24.3	24.2	24.4	21.0	23.7	-0.1410	-0.1192
07	50	00	23.6	24.3	24.3	24.2	24.4	20.8	23.7	-0.1398	-0.1189

ADDENDUM II. Reduced Data, ISIMU-II Experiment

DATA SET NUMBER = 1

OBS.	HR.	MIN.	SEC.	ELLAPSED TIME (MIN)	AMBIENT TEMP	P-3 (PSI)	P-2 (PSI)
1	11	52	10	0.00	24.3	-.4003	.4358
2	11	52	20	.17	24.3	-.2620	.4358
3	11	52	30	.33	24.2	1.0542	.4358
4	11	52	40	.50	24.3	1.4640	.4358
5	11	52	50	.67	24.3	1.6244	.4358
6	11	53	0	.83	24.3	1.6787	.4358
7	11	53	10	1.00	24.3	1.6851	.4358
8	11	53	20	1.17	24.3	1.6676	.4358
9	11	53	30	1.33	24.3	1.6400	.4358
10	11	53	40	1.50	24.3	1.6076	.4358
11	11	53	50	1.67	24.3	1.5732	.4358
12	11	54	0	1.83	24.3	1.5388	.4358
13	11	54	10	2.00	24.3	1.5056	.4358
14	11	54	20	2.17	24.3	1.4736	.4358
15	11	54	30	2.33	24.3	1.4425	.4358
16	11	54	40	2.50	24.3	1.4137	.4358
17	11	54	50	2.67	24.3	1.3861	.4358
18	11	55	0	2.83	24.3	1.3597	.4358
19	11	55	10	3.00	24.3	1.3345	.4358
20	11	55	20	3.17	24.3	1.3105	.4358
21	11	55	30	3.33	24.3	1.2881	.4358
22	11	55	40	3.50	24.3	1.2669	.4354
23	11	55	50	3.67	24.2	1.2461	.4354
24	11	56	0	3.83	24.3	1.2270	.4354
25	11	56	10	4.00	24.2	1.2082	.4354
26	11	56	20	4.17	24.3	1.1906	.4354
27	11	56	30	4.33	24.2	1.1738	.4354
28	11	56	40	4.50	24.2	1.1574	.4354
29	11	56	50	4.67	24.2	1.1414	.4354
30	11	57	0	4.83	24.3	1.1266	.4354
31	11	57	10	5.00	24.3	1.1122	.4354
32	11	57	20	5.17	24.3	1.0986	.4354
33	11	57	30	5.33	24.3	1.0850	.4358
34	11	57	40	5.50	24.3	1.0725	.4354
35	11	57	50	5.67	24.3	1.0598	.4354
36	11	58	0	5.83	24.3	1.0478	.4354
37	11	58	10	6.00	24.3	1.0362	.4354
38	11	58	20	6.17	24.3	1.0246	.4354
39	11	58	30	6.33	24.3	1.0134	.4354
40	11	58	40	6.50	24.3	1.0031	.4354
41	11	58	50	6.67	24.3	.9931	.4354
42	11	59	0	6.83	24.2	.9827	.4350
43	11	59	10	7.00	24.3	.9735	.4354
44	11	59	20	7.17	24.3	.9643	.4354
45	11	59	30	7.33	24.3	.9547	.4350
46	11	59	40	7.50	24.3	.9459	.4350
47	12	1	0	8.83	24.3	.8827	.4350
48	12	6	0	13.83	24.3	.7188	.4346
49	12	11	0	18.83	24.2	.6140	.4342
50	12	16	0	23.83	24.0	.5377	.4346
51	12	21	0	28.83	23.7	.4781	.4350
52	12	26	0	33.83	23.5	.4305	.4354
53	12	31	0	38.83	23.6	.3909	.4354
54	12	36	0	43.83	24.0	.3577	.4350
55	12	41	0	48.83	24.2	.3282	.4346

56	12	46	0	53.83	24.1	.3030	.4338
57	12	51	0	58.83	24.2	.2802	.4354
58	12	56	0	63.83	24.2	.2590	.4354
59	13	1	0	68.83	24.2	.2418	.4354
60	13	6	0	73.83	24.4	.2262	.4394
61	13	11	0	78.83	24.4	.2118	.4394
62	13	16	0	83.83	24.0	.1982	.4398
63	13	21	0	88.83	23.8	.1882	.4406
64	13	26	0	93.83	23.7	.1786	.4406
65	13	31	0	98.83	23.6	.1702	.4410
66	13	36	0	103.83	23.5	.1626	.4414
67	13	41	0	108.83	23.5	.1562	.4418
68	13	46	0	113.83	23.4	.1506	.4426
69	13	51	0	118.83	23.6	.1442	.4426
70	13	56	0	123.83	23.8	.1394	.4418
71	14	1	0	128.83	23.9	.1326	.4414
72	14	6	0	133.83	23.5	.1278	.4406
73	14	11	0	138.83	23.6	.1266	.4398
74	14	16	0	143.83	23.9	.1714	.4398
75	14	21	0	148.83	23.9	.1346	.4394
76	14	23	59	151.82	24.0	.1262	.4386
77	14	24	20	152.17	23.9	.1250	.4390
78	14	24	40	152.50	24.0	.1238	.4386
79	14	25	0	152.83	23.9	.1234	.4390
80	14	25	20	153.17	23.9	.1226	.4386
81	14	25	40	153.50	23.9	.1222	.4386
82	14	26	0	153.83	23.9	.1219	.4386
83	14	26	20	154.17	23.9	.1203	.4386
84	14	26	50	154.67	23.9	.1203	.4386
85	14	27	30	155.33	23.7	.1199	.4390
86	14	28	0	155.83	23.7	.1187	.4386

DATA SET NUMBER = 2

OBS.	HR.	MIN.	SEC.	ELLAPSED TIME (MIN)	AMBIENT TEMP	P-3 (PSI)	P-2 (PSI)
87	14	28	10	155.83	23.7	.7183	.4386
88	14	28	20	156.00	23.6	.5393	.4386
89	14	28	30	156.17	23.6	.5864	.4390
90	14	28	40	156.33	23.6	.6572	.4386
91	14	28	50	156.50	23.6	.7052	.4386
92	14	29	0	156.67	23.5	.7388	.4386
93	14	29	10	156.83	23.5	.7636	.4386
94	14	29	20	157.00	23.5	.7804	.4386
95	14	29	30	157.17	23.5	.7971	.4386
96	14	29	40	157.33	23.5	.8079	.4390
97	14	29	50	157.50	23.5	.8159	.4390
98	14	30	0	157.67	23.4	.8227	.4390
99	14	30	10	157.83	23.4	.8279	.4390
100	14	30	20	158.00	23.4	.8319	.4390
101	14	30	30	158.17	23.4	.8355	.4390
102	14	30	40	158.33	23.5	.8383	.4386
103	14	30	50	158.50	23.4	.8403	.4390
104	14	31	0	158.67	23.4	.8407	.4390
105	14	31	10	158.83	23.4	.8419	.4386
106	14	31	20	159.00	23.3	.8427	.4390
107	14	31	30	159.17	23.3	.8435	.4390
108	14	31	50	159.50	23.3	.8435	.4386
109	14	32	0	159.67	23.3	.8427	.4390
110	14	32	10	159.83	23.3	.8423	.4386
111	14	32	20	160.00	23.3	.8411	.4386
112	14	32	30	160.17	23.3	.8399	.4386
113	14	32	40	160.33	23.3	.8395	.4390
114	14	32	50	160.50	23.3	.8383	.4390
115	14	33	0	160.67	23.8	.8375	.4390
116	14	33	10	160.83	23.7	.8363	.4386
117	14	33	20	161.00	23.6	.8351	.4390
118	14	33	30	161.17	23.5	.8335	.4386
119	14	33	40	161.33	23.5	.8323	.4390
120	14	33	50	161.50	23.5	.8303	.4386
121	14	34	0	161.67	23.5	.8291	.4390
122	14	34	10	161.83	23.4	.8267	.4386
123	14	34	20	162.00	23.4	.8255	.4390
124	14	34	30	162.17	23.4	.8243	.4390
125	14	34	40	162.33	23.3	.8223	.4390
126	14	34	50	162.50	23.3	.8211	.4390
127	14	35	0	162.67	23.3	.8191	.4390
128	14	35	10	162.83	23.3	.8175	.4390
129	14	35	20	163.00	23.3	.8159	.4390
130	14	35	30	163.17	23.3	.8151	.4390
131	14	35	40	163.33	23.3	.8139	.4390
132	14	35	50	163.50	23.2	.8115	.4390
133	14	36	0	163.67	23.2	.8095	.4390
134	14	36	10	163.83	23.2	.8079	.4390
135	14	36	20	164.00	23.3	.8059	.4394
136	14	36	30	164.17	23.2	.8039	.4390
137	14	36	40	164.33	23.1	.8027	.4390
138	14	36	50	164.50	23.1	.8011	.4394
139	14	37	0	164.67	23.1	.7987	.4390
140	14	37	10	164.83	23.1	.7975	.4394
141	14	37	20	165.00	23.1	.7963	.4394

142	14	37	30	165.17	23.1	.7943	.4394
143	14	37	40	165.33	23.0	.7919	.4394
144	14	37	50	165.50	23.0	.7907	.4394
145	14	38	0	165.67	23.0	.7887	.4394
146	14	38	10	165.83	23.1	.7872	.4394
147	14	38	20	166.00	23.1	.7852	.4394
148	14	38	30	166.17	23.0	.7836	.4394
149	14	38	40	166.33	23.0	.7816	.4394
150	14	38	50	166.50	23.0	.7800	.4394
151	14	39	0	166.67	23.0	.7784	.4398
152	14	39	10	166.83	23.0	.7764	.4398
153	14	39	20	167.00	23.0	.7744	.4394
154	14	39	30	167.17	23.0	.7728	.4394
155	14	39	40	167.33	23.0	.7704	.4394
156	14	39	50	167.50	23.0	.7684	.4398
157	14	40	5	167.75	23.0	.7660	.4398
158	14	41	0	168.67	22.9	.7564	.4394
159	14	46	0	173.67	22.8	.7064	.4398
160	14	51	0	178.67	22.6	.6620	.4406
161	14	56	0	183.67	22.5	.6228	.4410
162	15	1	0	188.67	22.4	.5876	.4418
163	15	6	0	193.67	22.4	.5569	.4425
164	15	11	0	198.67	22.2	.5273	.4430
165	15	16	0	203.67	22.3	.5017	.4438
166	15	21	0	208.67	22.4	.4773	.4438
167	15	26	0	213.67	22.8	.4557	.4438
168	15	31	0	218.67	22.9	.4353	.4430
169	15	36	0	223.67	22.8	.4165	.4425
170	15	41	0	228.67	22.9	.3985	.4418
171	15	46	0	233.67	23.2	.3821	.4414
172	15	51	0	238.67	23.1	.3653	.4406
173	15	56	0	243.67	22.9	.3513	.4406
174	16	1	0	248.67	23.0	.3374	.4406
175	16	6	0	253.67	23.2	.3242	.4398
176	16	11	0	258.67	22.8	.3122	.4398
177	16	16	0	263.67	22.5	.3002	.4402
178	16	18	42	266.37	22.6	.2950	.4402
179	16	18	56	266.60	22.6	.2938	.4406
180	16	24	9	271.82	22.5	.2842	.4406
181	16	30	0	277.67	22.4	.2730	.4414
182	16	40	0	287.67	22.2	.2570	.4422
183	16	50	0	297.67	22.4	.2426	.4422
184	17	0	0	307.67	23.1	.2278	.4414
185	17	10	0	317.67	23.4	.2126	.4398
186	17	20	0	327.67	23.4	.1978	.4394
187	17	30	0	337.67	23.5	.1842	.4386
188	17	40	0	347.67	23.6	.1722	.4378
189	17	50	0	357.67	23.6	.1602	.4374
190	18	0	0	367.67	23.7	.1494	.4370
191	18	10	0	377.67	23.7	.1398	.4366
192	18	20	0	387.67	23.8	.1310	.4366
193	18	30	0	397.67	23.8	.1222	.4362
194	18	40	0	407.67	23.7	.1143	.4362
195	18	50	0	417.67	23.8	.1075	.4358
196	19	0	0	427.67	23.9	.1007	.4354
197	19	10	0	437.67	23.9	.0939	.4358
198	19	20	0	447.67	23.9	.0883	.4354
199	19	30	0	457.67	24.0	.0835	.4354
200	19	40	0	467.67	24.0	.0787	.4354
201	19	50	0	477.67	23.9	.0747	.4358
202	20	0	0	487.67	23.8	.0707	.4358

203	20	10	0	497.67	23.9	.0667	.4358
204	20	20	0	507.67	23.9	.0627	.4358
205	20	30	0	517.67	24.0	.0591	.4354
206	20	40	0	527.67	24.0	.0555	.4354
207	20	50	0	537.67	23.9	.0523	.4354
208	21	0	0	547.67	23.9	.0499	.4358
209	21	10	0	557.67	23.9	.0471	.4358
210	21	20	0	567.67	23.9	.0447	.4358
211	21	30	0	577.67	23.8	.0435	.4358
212	21	40	0	587.67	23.8	.0419	.4358
213	21	50	0	597.67	23.9	.0407	.4362
214	22	0	0	607.67	23.8	.0391	.4362
215	22	10	0	617.67	24.0	.0367	.4362
216	22	20	0	627.67	24.0	.0351	.4362
217	22	30	0	637.67	23.9	.0331	.4358
218	22	40	0	647.67	24.0	.0315	.4358
219	22	50	0	657.67	24.0	.0299	.4358
220	23	0	0	667.67	23.9	.0291	.4358
221	23	10	0	677.67	23.9	.0287	.4362
222	23	20	0	687.67	23.9	.0275	.4390
223	23	30	0	697.67	23.8	.0267	.4366
224	23	40	0	707.67	23.8	.0259	.4366
225	23	50	0	717.67	23.8	.0251	.4366
226	24	20	0	747.67	23.7	.0251	.4370
227	24	50	0	777.67	23.5	.0255	.4370
228	25	20	0	807.67	23.5	.0259	.4374
229	25	50	0	837.67	23.4	.0267	.4374
230	26	20	0	867.67	23.3	.0275	.4378
231	26	50	0	897.67	23.3	.0283	.4382
232	27	20	0	927.67	23.2	.0295	.4382
233	27	50	0	957.67	22.9	.0307	.4386
234	28	20	0	987.67	22.9	.0327	.4390
235	28	50	0	1017.67	22.9	.0343	.4386
236	29	20	0	1047.67	22.7	.0355	.4390
237	29	50	0	1077.67	22.7	.0367	.4394
238	30	20	0	1107.67	22.9	.0387	.4390
239	30	40	0	1127.67	22.0	.0471	.4474
240	30	50	0	1137.67	22.9	.0551	.4470
241	31	0	0	1147.67	22.6	.0571	.4450
242	31	30	0	1177.67	22.0	.0575	.4438
243	32	0	0	1207.67	23.1	.0555	.4410
244	32	20	0	1227.67	22.8	.0579	.4398

DATA SET NUMBER = 3

OBS.	HR.	MIN.	SEC.	ELLAPSED TIME (MIN)	AMBIENT TEMP	P-3 (PSI)	P-2 (PSI)
245	9	24	20	1227.67	23.5	.0511	-.4355
246	9	24	30	1227.83	23.5	.0571	-.2270
247	9	24	40	1228.00	23.5	.0967	1.3107
248	9	24	50	1228.17	23.5	.1183	1.4270
249	9	25	0	1228.33	23.5	.1346	1.4421
250	9	25	10	1228.50	23.5	.1466	1.4354
251	9	25	20	1228.67	23.5	.1562	1.4198
252	9	25	30	1228.83	23.5	.1634	1.4002
253	9	25	40	1229.00	23.5	.1690	1.3790
254	9	25	50	1229.17	23.5	.1738	1.3578
255	9	26	0	1229.33	23.5	.1778	1.3367
256	9	26	10	1229.50	23.5	.1802	1.3155
257	9	26	20	1229.67	23.5	.1825	1.2955
258	9	26	30	1229.83	23.4	.1846	1.2764
259	9	26	40	1230.00	23.5	.1862	1.2576
260	9	26	50	1230.17	23.5	.1870	1.2396
261	9	27	0	1230.33	23.5	.1882	1.2224
262	9	27	10	1230.50	23.5	.1886	1.2056
263	9	27	20	1230.67	23.5	.1890	1.1901
264	9	27	30	1230.83	23.5	.1894	1.1745
265	9	27	40	1231.00	23.5	.1898	1.1601
266	9	27	50	1231.17	23.5	.1898	1.1457
267	9	28	0	1231.33	23.5	.1898	1.1305
268	9	28	10	1231.50	23.5	.1902	1.1170
269	9	28	20	1231.67	23.5	.1902	1.1038
270	9	28	30	1231.83	23.5	.1902	1.0918
271	9	28	40	1232.00	23.5	.1902	1.0798
272	9	28	50	1232.17	23.5	.1898	1.0686
273	9	29	0	1232.33	23.5	.1898	1.0574
274	9	29	10	1232.50	23.5	.1894	1.0462
275	9	29	20	1232.67	23.5	.1894	1.0359
276	9	29	30	1232.83	23.5	.1894	1.0259
277	9	29	40	1233.00	23.5	.1894	1.0159
278	9	29	50	1233.17	23.5	.1890	1.0059
279	9	30	0	1233.33	23.5	.1890	.9971
280	9	30	10	1233.50	23.5	.1886	.9879
281	9	30	20	1233.67	23.5	.1886	.9791
282	9	30	30	1233.83	23.6	.1886	.9707
283	9	30	40	1234.00	23.5	.1882	.9619
284	9	30	50	1234.17	23.5	.1878	.9540
285	9	31	0	1234.33	23.5	.1882	.9460
286	9	31	10	1234.50	23.5	.1878	.9384
287	9	31	20	1234.67	23.4	.1874	.9304
288	9	31	30	1234.83	23.5	.1874	.9228
289	9	31	40	1235.00	23.5	.1874	.9156
290	9	31	50	1235.17	23.4	.1874	.9084
291	9	32	0	1235.33	23.4	.1874	.9012
292	9	32	10	1235.50	23.4	.1870	.8948
293	9	32	20	1235.67	23.4	.1870	.8880
294	9	32	30	1235.83	23.4	.1866	.8816
295	9	32	40	1236.00	23.3	.1866	.8749
296	9	32	50	1236.17	23.3	.1866	.8685
297	9	33	0	1236.33	23.3	.1866	.8625
298	9	33	10	1236.50	23.2	.1866	.8565
299	9	33	20	1236.67	23.2	.1862	.8501

300	9	33	30	1236.83	23.2	.1862	.8441
301	9	33	40	1237.00	23.1	.1862	.8385
302	9	33	50	1237.17	23.1	.1862	.8333
303	9	34	0	1237.33	23.1	.1858	.8277
304	9	34	10	1237.50	23.0	.1858	.8221
305	9	34	20	1237.67	23.0	.1858	.8169
306	9	34	30	1237.83	22.9	.1854	.8109
307	9	34	40	1238.00	22.9	.1854	.8057
308	9	34	50	1238.17	23.0	.1854	.8005
309	9	35	0	1238.33	22.8	.1854	.7958
310	9	35	10	1238.50	22.8	.1854	.7906
311	9	35	20	1238.67	22.8	.1854	.7858
312	9	35	30	1238.83	22.8	.1850	.7806
313	9	35	40	1239.00	22.7	.1850	.7752
314	9	35	50	1239.17	22.8	.1850	.7714
315	9	36	0	1239.33	22.7	.1850	.7670
316	9	36	10	1239.50	22.7	.1846	.7626
317	9	40	0	1243.33	22.2	.1834	.6719
318	9	45	0	1248.33	22.3	.1818	.5828
319	9	50	0	1253.33	23.0	.1786	.5121
320	9	55	0	1258.33	23.2	.1746	.4546
321	10	0	0	1263.33	23.3	.1694	.4066
322	10	5	0	1268.33	23.4	.1646	.3671
323	10	10	0	1273.33	23.4	.1590	.3319
324	10	15	0	1278.33	23.5	.1534	.3028
325	10	20	0	1283.33	23.1	.1486	.2775
326	10	25	0	1288.33	22.4	.1438	.2544
327	10	30	0	1293.33	22.1	.1390	.2337
328	10	35	0	1298.33	22.5	.1362	.2153
329	10	40	0	1303.33	22.9	.1318	.1989
330	10	45	0	1308.33	23.2	.1278	.1841
331	10	50	0	1313.33	23.3	.1238	.1709
332	10	55	0	1318.33	23.4	.1195	.1590
333	11	0	0	1323.33	23.4	.1155	.1486
334	11	5	0	1328.33	23.5	.1119	.1398
335	11	10	0	1333.33	23.7	.1079	.1294
336	11	15	0	1338.33	23.1	.1043	.1210
337	11	20	0	1343.33	22.7	.1011	.1130
338	11	20	30	1343.83	22.7	.1007	.1126
339	11	21	30	1344.83	22.5	.0999	.1114
340	11	22	30	1345.83	22.6	.0995	.1098

DATA SET NUMBER = 4

OBS.	HR.	MIN.	SEC.	ELLAPSED TIME (MIN)	AMBIENT TEMP	P-3 (PSI)	P-2 (PSI)
341	11	23	0	1345.83	22.7	.0991	.1102
342	11	23	30	1346.33	22.4	.0995	.1086
343	11	24	0	1346.83	22.2	.0979	.1082
344	11	24	30	1347.33	22.8	.0947	.1062
345	11	25	0	1347.83	22.1	.0967	.1050
346	11	25	30	1348.33	22.5	.0935	.1038
347	11	26	0	1348.83	22.7	.0947	.1034
348	11	27	0	1349.83	22.3	.0971	.1018
349	11	28	0	1350.83	22.3	.1003	.1022
350	11	29	0	1351.83	22.0	.1039	.1042
351	11	30	0	1352.83	22.0	.1083	.1046
352	11	31	0	1353.83	22.2	.1119	.1054
353	11	32	0	1354.83	22.2	.1167	.1074
354	11	33	0	1355.83	22.4	.1195	.1110
355	11	34	0	1356.83	22.0	.1242	.1126
356	11	35	0	1357.83	22.4	.1294	.1142
357	11	36	0	1358.83	22.6	.1318	.1166
358	11	37	0	1359.83	22.9	.1354	.1194
359	11	39	0	1361.83	23.0	.1430	.1222
360	11	41	0	1363.83	22.9	.1478	.1258
361	11	43	0	1365.83	23.3	.1542	.1294
362	11	45	0	1367.83	23.9	.1566	.1330
363	11	47	0	1369.83	23.8	.1602	.1366
364	11	50	0	1372.83	23.9	.1658	.1410
365	11	54	0	1376.83	24.1	.1726	.1446
366	11	57	0	1379.83	23.4	.1774	.1494
367	12	7	0	1389.83	24.3	.1854	.1542
368	12	19	0	1401.83	22.3	.1926	.1590
369	12	31	0	1413.83	22.0	.1986	.1597
370	12	39	0	1421.83	22.7	.1998	.1578
371	12	49	0	1431.83	22.3	.2018	.1534
372	12	59	0	1441.83	23.4	.1998	.1506
373	13	14	0	1456.83	22.8	.1974	.1438
374	13	24	0	1466.83	23.5	.1922	.1382
375	13	34	0	1476.83	23.7	.1866	.1366
376	13	44	0	1486.83	22.7	.1846	.1330
377	13	54	0	1496.83	23.2	.1810	.1266
378	14	4	0	1506.83	22.5	.1794	.1226
379	14	14	0	1516.83	22.5	.1758	.1186
380	14	24	0	1526.83	22.3	.1726	.1142
381	14	34	0	1536.83	23.0	.1590	.1114
382	14	44	0	1546.83	22.7	.1654	.1094
383	14	54	0	1556.83	22.5	.1638	.1058
384	15	4	0	1566.83	22.3	.1602	.1014
385	15	14	0	1576.83	22.9	.1554	.0982
386	15	24	0	1586.83	22.6	.1538	.0966
387	15	34	0	1596.83	23.2	.1498	.0934

ADDENDUM III. Excess Pore Pressure Prediction Program MENUDO

```
10 ! PROGRAM "MENUDO"
20 ! THIS PROGRAM PLOTS CALCULATES EXPECTANT PORE PRESSURES BASED ON THERMAL AND
 TIME EFFECTS
30 OPTION BASE 1
40 ! PRINTER IS 701,80
50 DIM M(50),T(50),U1(50),U2(50),U3(50),U4(50),X(50),Y1(50),Y2(50)
60 DIM D(50),T4(50),U(50),P(50)
70 M=8
80 N=47
90 ! A1&B1 ARE CURVE FIT PARAMETERS FOR TEMP.=f(TIME) RELATIONSHIP
100 A1=210
110 B1=.25
120 ! T0=INITIAL TEMPERATURE
130 T0=22.8
140 ! N1=INITIAL POROSITY
150 N1=.74
160 ! A2=THERMAL COEFFICIENT OF EXPANSION FOR SOIL SOLIDS
170 A2=.000001
180 ! A3=THERMAL COEFFICIENT OF EXPANSION FOR SOIL STRUCTURE
190 A3=-.00005 PER °C
200 ! M1=Mvs COEFFICIENT OF VERTICAL COMPRESSIBILITY FOR REBOUND
210 M1=-.00025
220 ! C1=Cv COEFFICIENT OF CONSOLIDATION/HYDRAULIC DIFFUSIVITY
230 ! FOR PROBE P-3 IN CM^2/MIN
240 C1=.019277
250 ! FOR PROBE P-2 IN CM^2/MIN
260 ! C1=.014035
270 ! R1=PROBE RADIUS
280 R1=.4
290 ! M2=SMEAR FACTOR/INTERFACE DISTURBANCE
300 ! FOR PROBE P-3
310 M2=4.6
320 ! FOR PROBE P-2
330 ! M2=2.3
340 ! PORE PRESSURE PARAMETERS DUE TO PREVIOUS HISTORY
350 ! FOR PROBE P-3
360 A4=.1898 @ B4=-.006193 @ T4=100
370 ! FOR PROBE P-2
380 ! A4=.5856 @ B4=-.01726 @ T4=100
390 C4=A4*EXP(B4*T4)
400 ! READS IN PREVIOUSLY STORED DATA
410 FOR Q=M TO N
420 ASSIGN# 1 TO "PROBEDATA4:D701"
430 READ# 1,Q : M(Q),T1,T2,T3,T4(Q),T5,T6,T7,U1(Q),U2(Q)
440 ASSIGN# 1 TO *
450 NEXT Q
460 GOTO 530
470 DISP "DO YOU WANT TO CHANGE A&B PARAMETERS Y/N" @ BEEP
480 INPUT B$
490 IF B$="N" THEN 1200
500 DISP "INPUT A&B" @ BEEP
510 INPUT A1,B1
520 PRINT A1;B1
530 D=0
540 U=0
550 FOR I=M TO N
560 D=D+1
570 X(D)=M(I)-M(M)
580 ! PROBE P-3 VOLTAGE-TO-PRESSURE CONVERSION
590 Y1(D)=.0111+(U1(I)+.1505)*3.9982
600 ! PROBE P-2 VOLTAGE-TO-PRESSURE CONVERSION
```

```
610 ! Y1(0)=.0391+(U2(I)+.1071)*3.995
620 ! TEMPERATURE AS A FUNCTION OF TIME
630 T(0)=X(0)/(A1+B1*X(0))+T0
640 ! A0=THERMAL COEFFICIENT OF EXPANSION FOR SEA WATER
650 A0=.000064809+.000010474*T(0)-.000000056*T(0)^2
660 IF 0=1 THEN T2=0 ELSE T2=T(0)-T(0-1)
670 ! U3=PORE PRESSURE INCREASE DUE TO THERMAL EFFECTS
680 U3(0)=T2/M1*(N1*(A2-A0)+A3)
690 ! U4=PORE PRESSURE INCREASE CORRECTION DUE TO PREVIOUS HISTORY
700 U4(0)=C4-A4*EXP(B4*(T4+X(0)))
710 U=U3(0)+U
720 U(0)=U+U4(0)
730 ! P1=PORE PRESSURE DISSIPATION AS A FUNCTION OF TIME
740 B0=-(C1/R1^2/M2)
750 P=0
760 FOR L=1 TO 0
770 IF L=1 THEN P1=0 ELSE P1=U3(L-1)*EXP(B0*(X(0)-X(L-1)))
780 P=P+P1
790 NEXT L
800 IF 0=1 THEN P(0)=Y1(1) ELSE P(0)=U3(0)+P+Y1(1)
810 IMAGE DD,2X,DDD.DD,2X,D.DDD ,2X, D.DDD,2X,D.DDD
820 ! PRINT USING 810 ; 0,X(0),Y1(0),U(0)+Y1(1),P(0)+Y1(1)
830 IMAGE D.DDDD,2X,D.DDDD,2X,D.DDD
840 ! PRINT USING 830 ; U3(0),U4(0),P(0)
850 ! PRINT
860 NEXT I
870 DEG
880 PLOTTER IS 705
890 LIMIT 10.230,10.180
900 LOCATE 10.125,10.95
910 SCALE 0.300,0.1.2
920 FXD 0.1
930 LAXES -25,,1,0.0.2,2
940 CSIZE 4
950 SETGU
960 MOVE 68.5 @ LORG 5
970 LABEL "TIME (MIN.)"
980 MOVE 3.53 @ LDIR 90
990 LABEL "PRESSURE (PSI)"
1000 SETUU @ LORG 2 @ LDIR 0
1010 MOVE 150,1.2 @ LABEL "PORE PRESSURE PROBE P-3"
1020 ! MOVE 150,1.2 @ LABEL "PORE PRESSURE PROBE P-2"
1030 MOVE 150,1.15 @ LABEL "* - DATA"
1040 MOVE 150,1.1 @ LABEL "+ - THERMALLY INDUCED PORE PRESSURE"
1050 MOVE 150,1.05 @ LABEL "O - THEORY PREDICTION"
1060 LORG 5 @ CSIZE 2
1070 FOR J=1 TO 0
1080 MOVE X(J),Y1(J)+U4(J)
1090 LABEL "*"
1100 NEXT J
1110 FOR K=1 TO 0
1120 MOVE X(K),U(K)-U4(K)+Y1(1)
1130 LABEL "+"
1140 NEXT K
1150 FOR L=1 TO 0
1160 MOVE X(L),P(L)
1170 LABEL "O"
1180 NEXT L
1190 GOTO 470
1200 DISP "ADIOS SENOR RIGONES"
1210 END
```

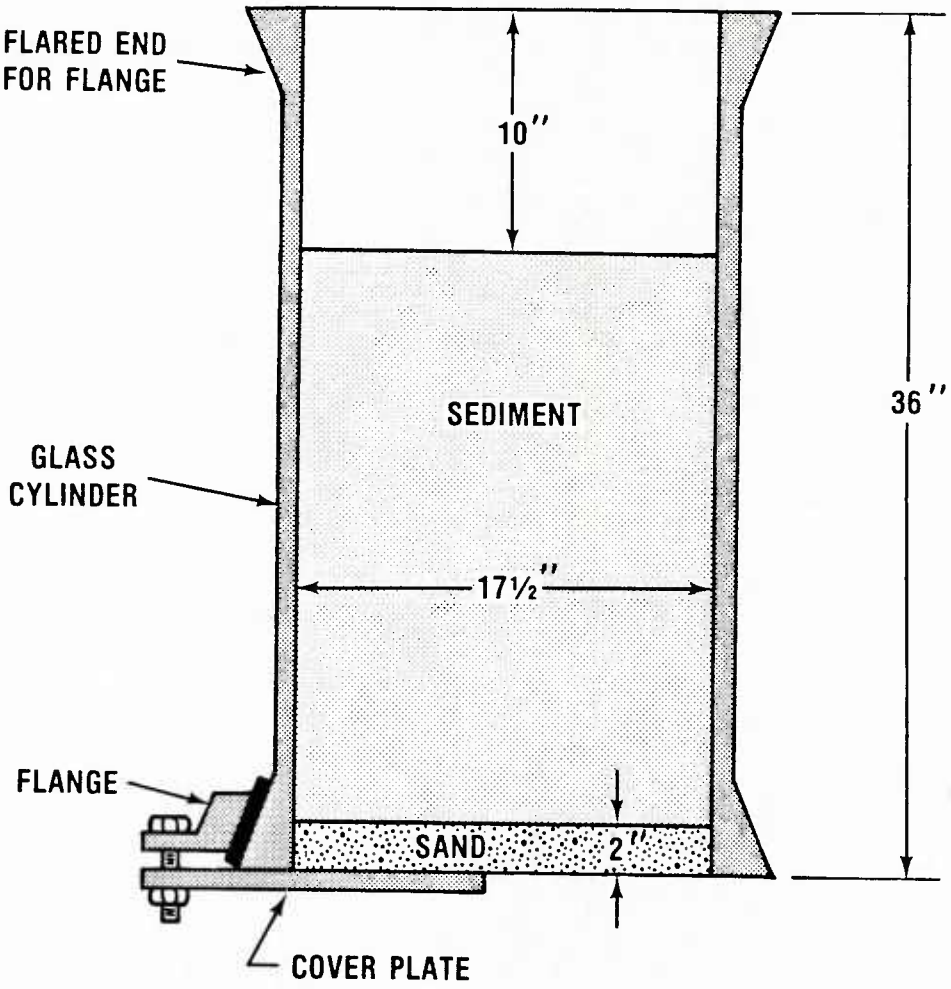

Figure 1. ARRANGEMENT FOR SEDIMENT CONSOLIDATION AT SNLA

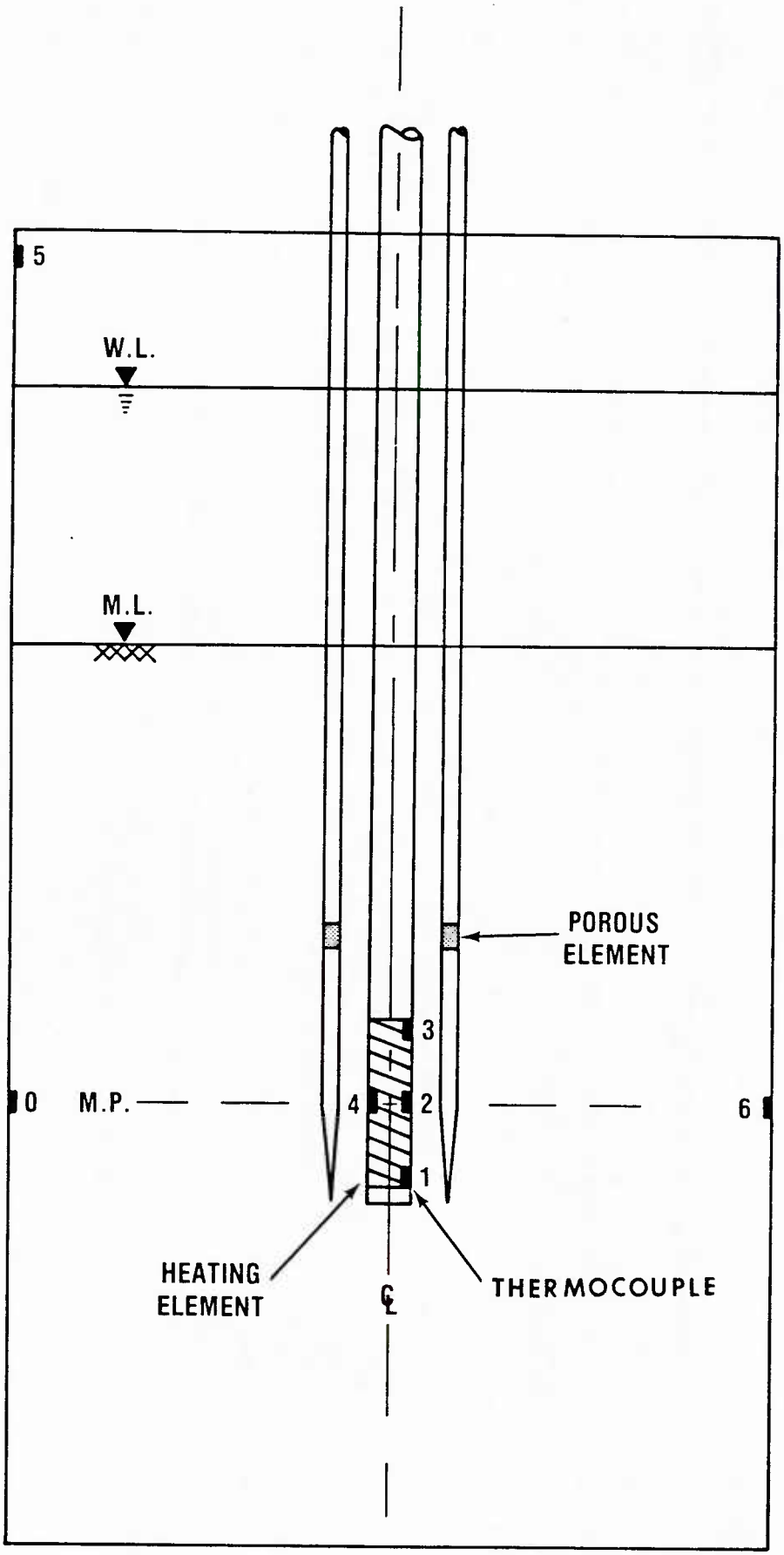

Figure 2. PLAN VIEW OF TEST ARRANGEMENT (SCALE 1 :4)

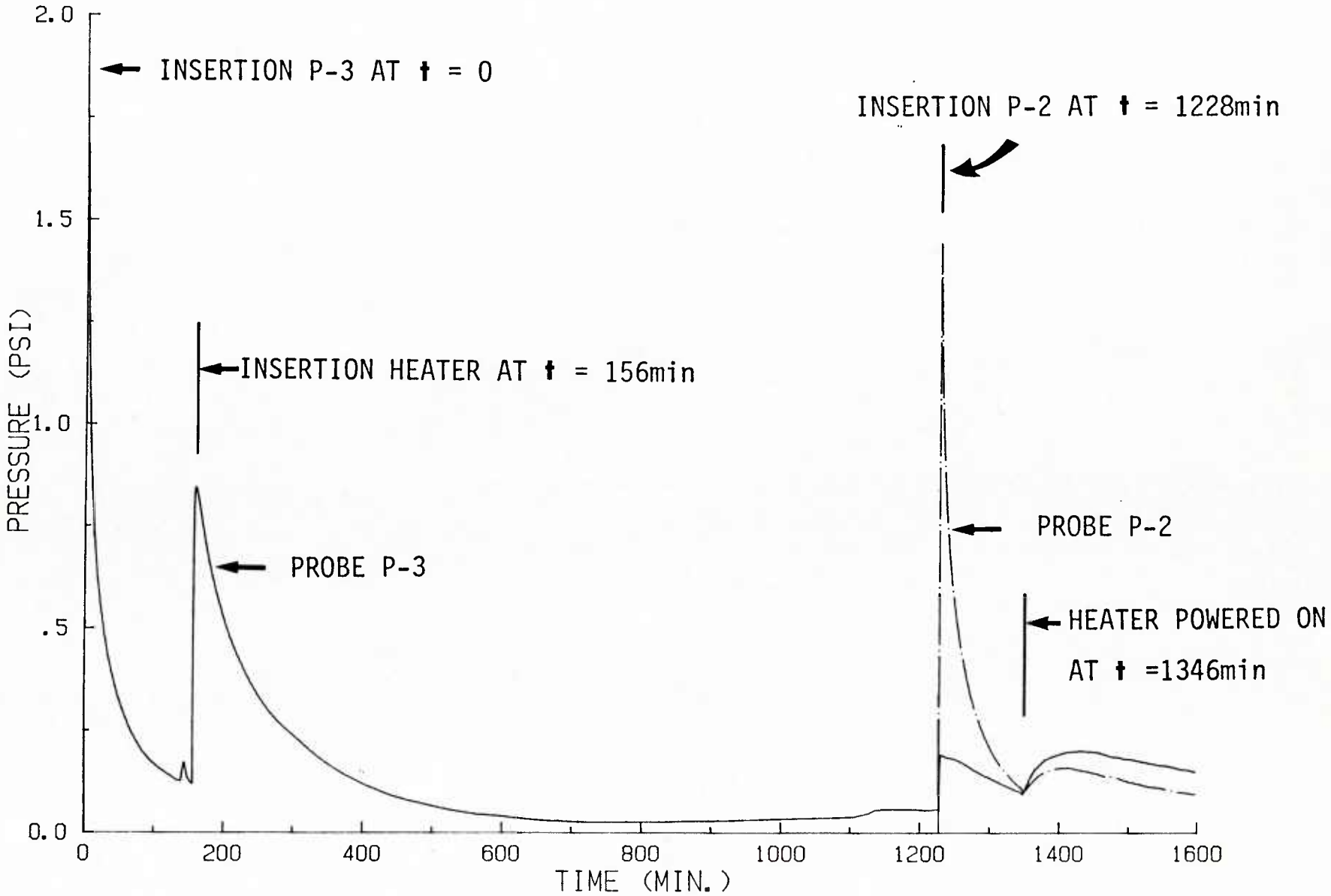

Figure 3. PIEZOMETER PORE PRESSURE RESPONSE FOR THE COMPLETE TEST PERIOD

(1psi = 6.895kPa)

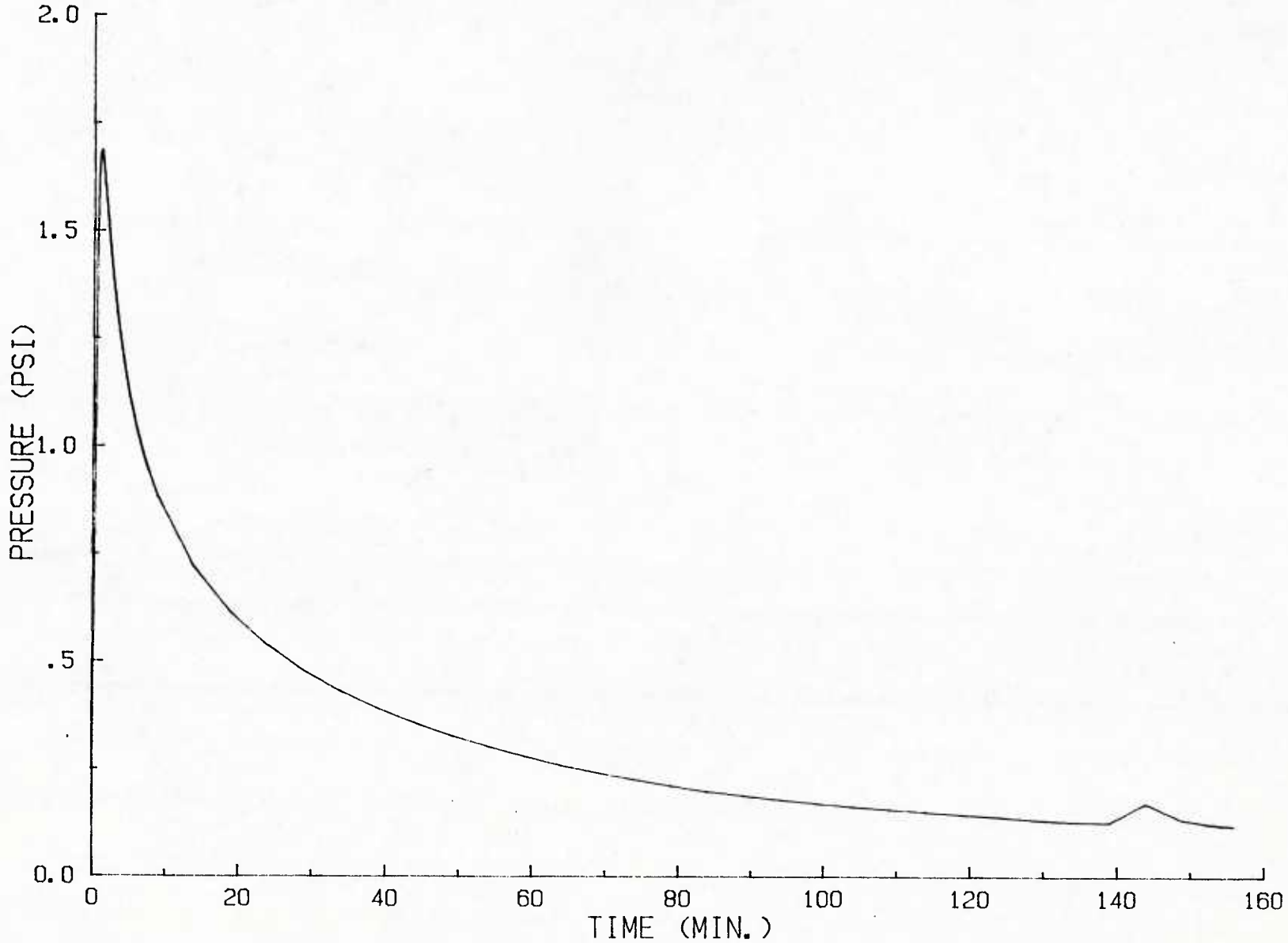

Figure 4. PIEZOMETER PORE PRESSURE RESPONSE DURING EVENT 1: PROBE P-3 INSERTION

(1psi = 6.895kPa)

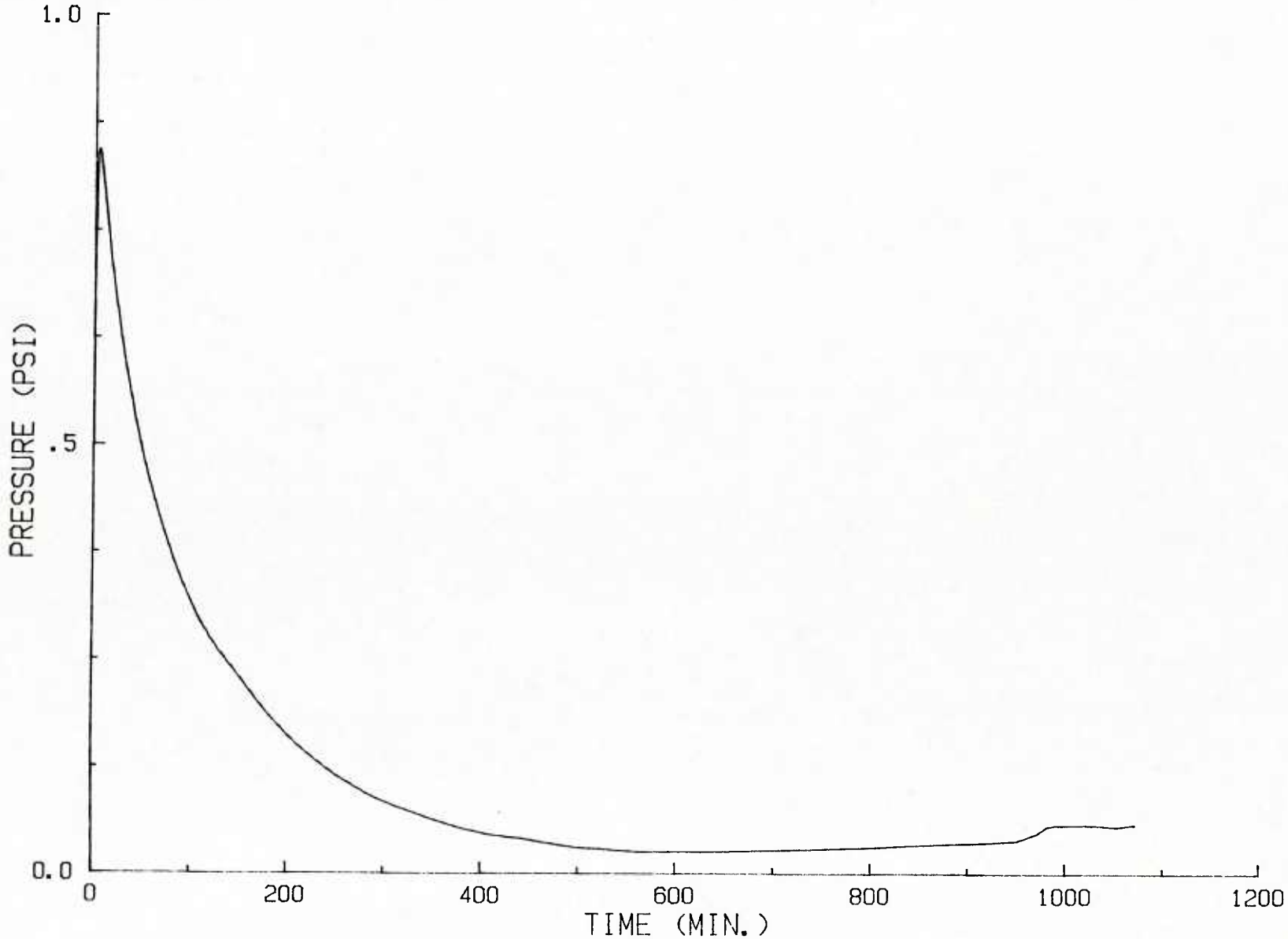

Figure 5. PIEZOMETER PORE PRESSURE RESPONSE AT PROBE P-3 DURING EVENT 2: HEATER INSERTION

(1psi = 6.895kPa)

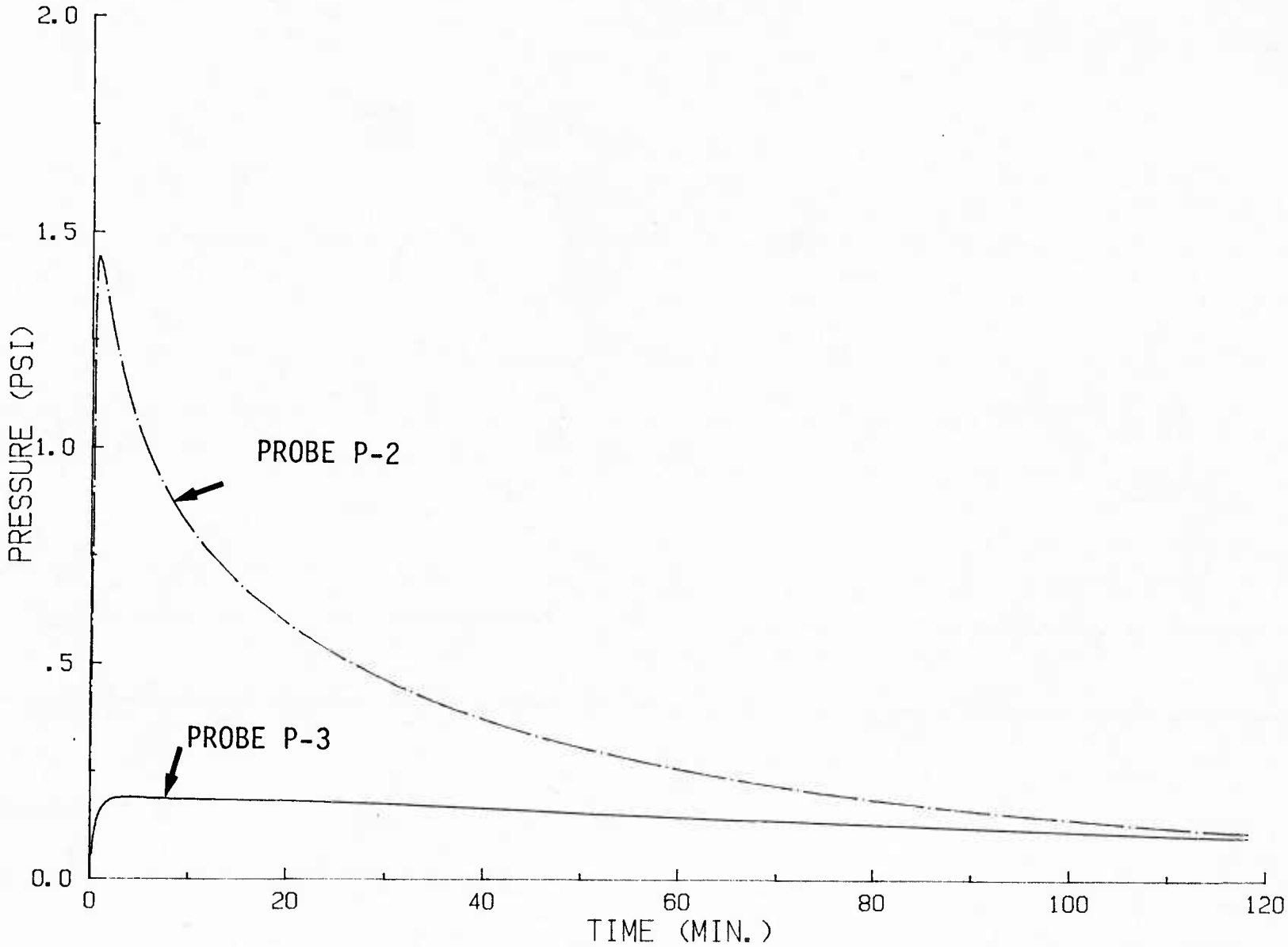

Figure 6. PIEZOMETER PORE PRESSURE RESPONSE DURING EVENT 3: PROBE P-2 INSERTION

(1 psi = 6.895kPa)

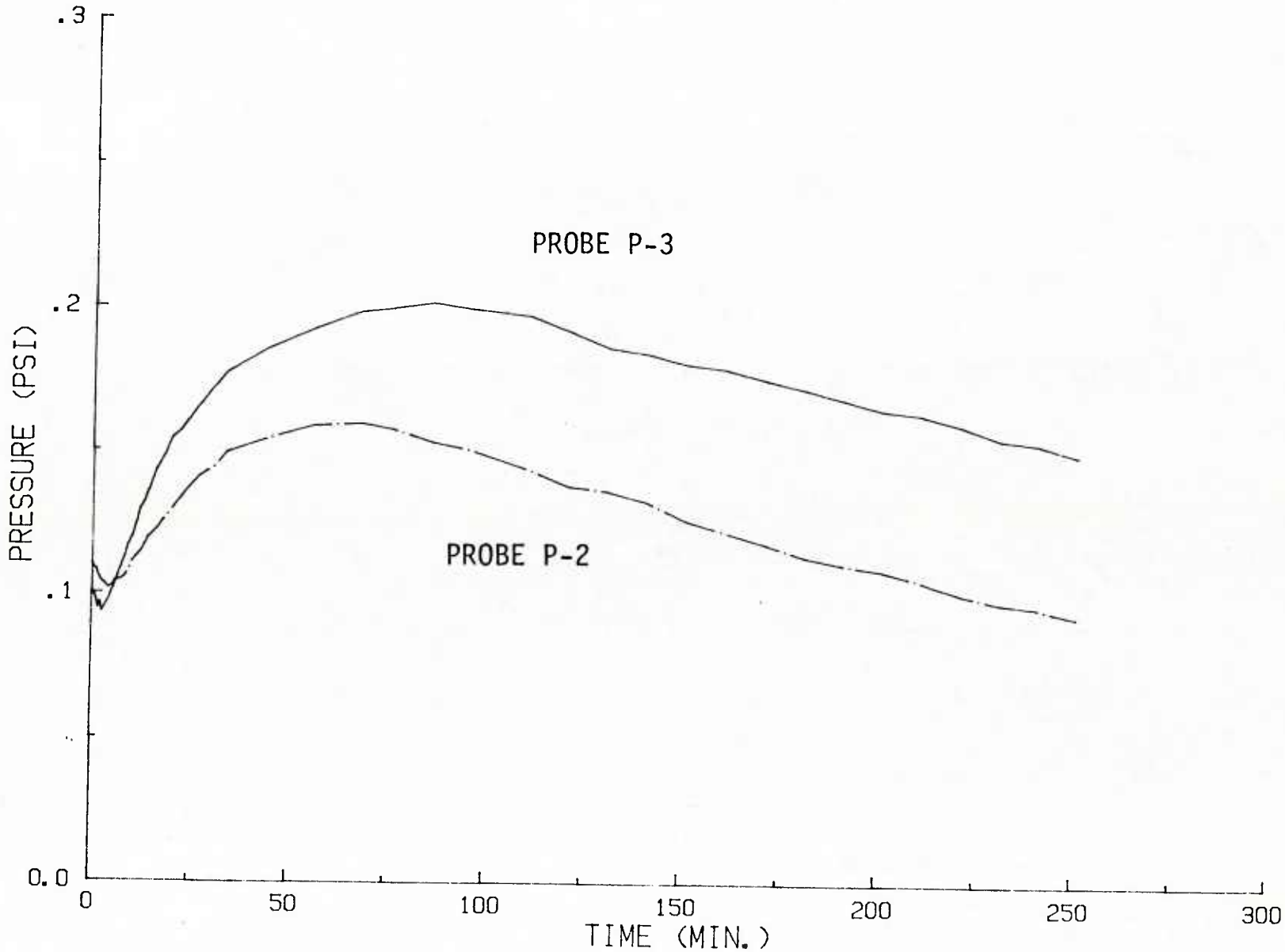

Figure 7. PIEZOMETER PORE PRESSURE RESPONSE DURING EVENT 4: HEATER ACTIVATION

(1psi = 6.895kPa)

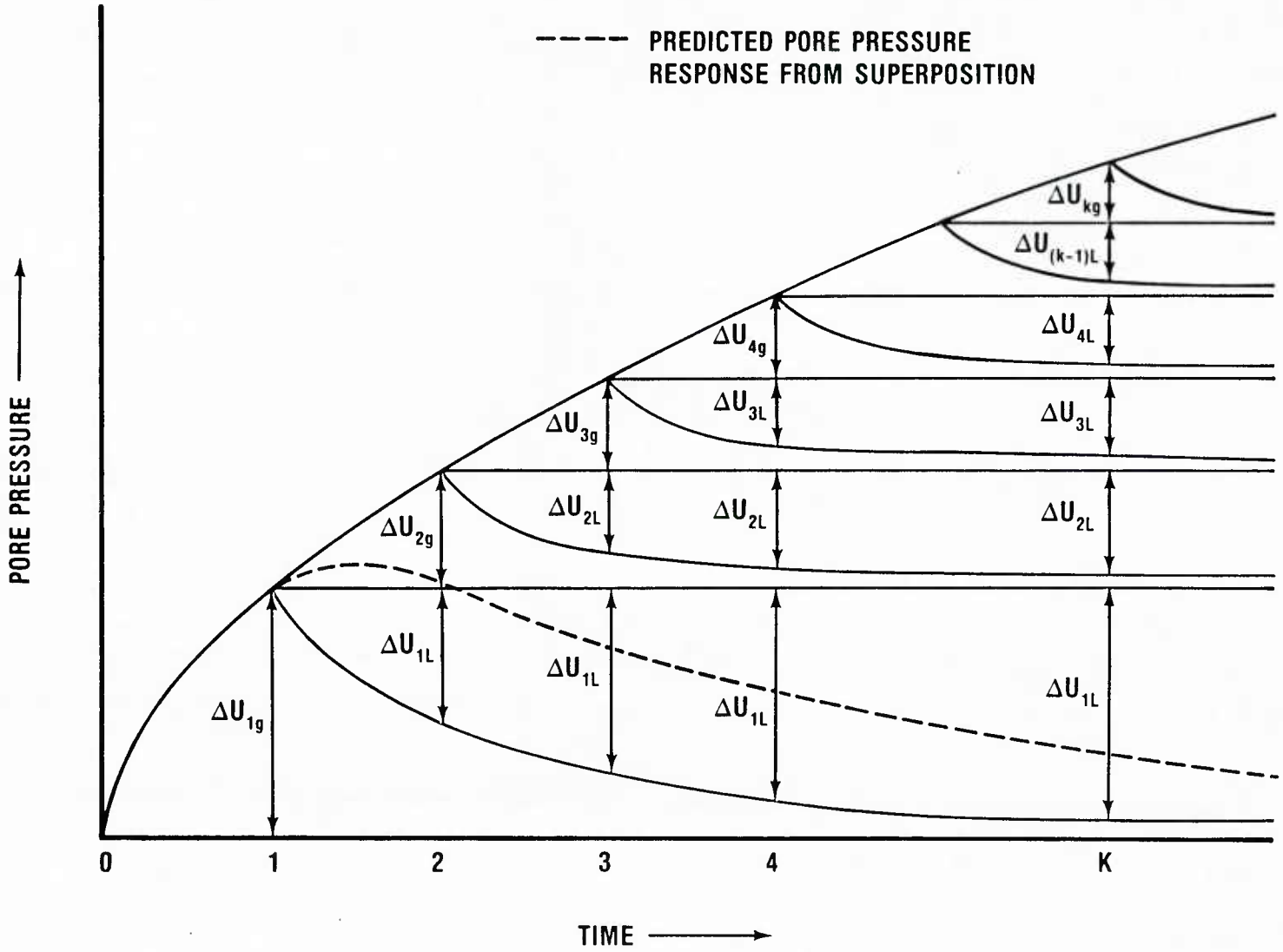

Figure 8. GRAPHICAL REPRESENTATION OF PORE PRESSURE GAIN-LOSS MODELS

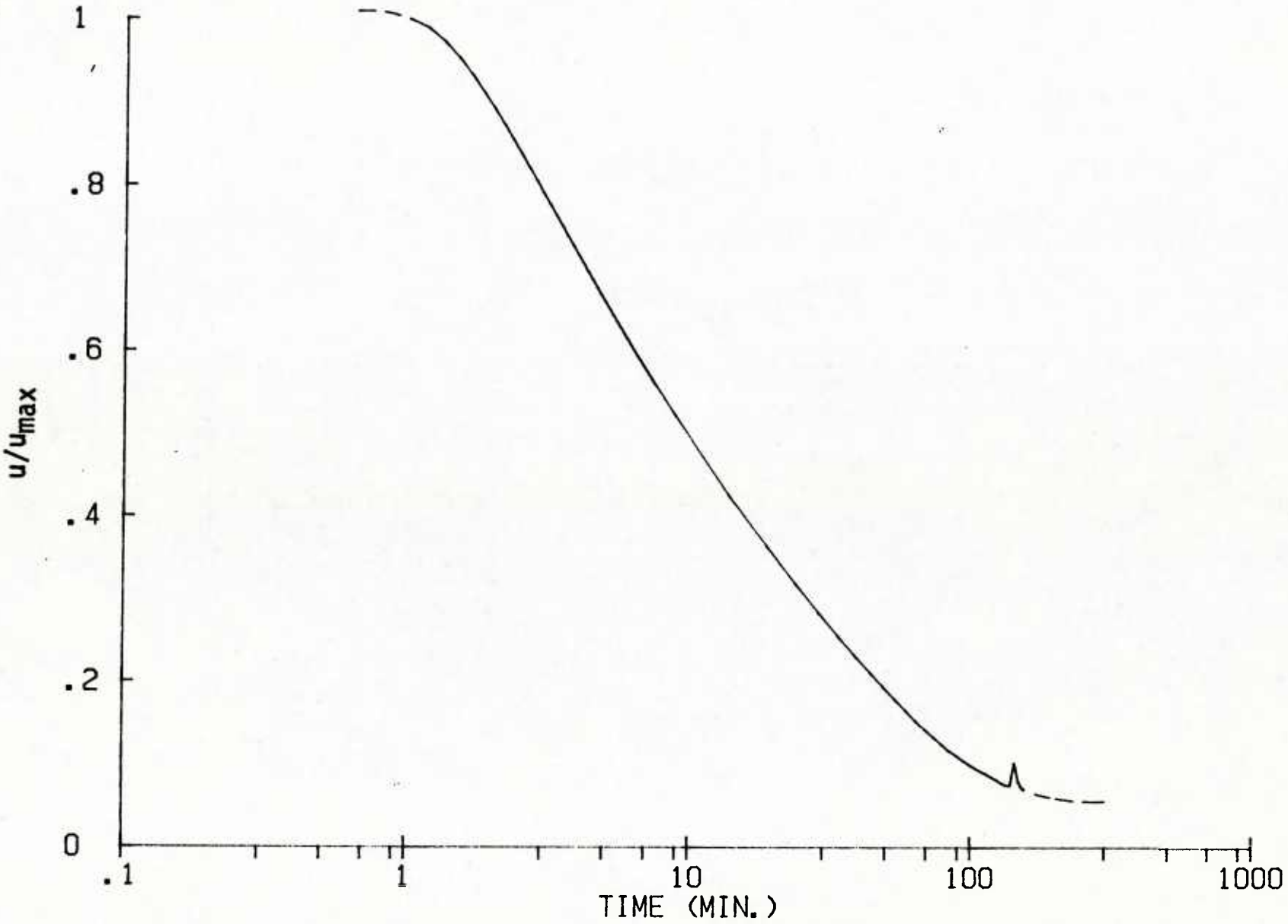

Figure 9. THE LOG (TIME) DISSIPATION CURVE FOR PROBE P-3

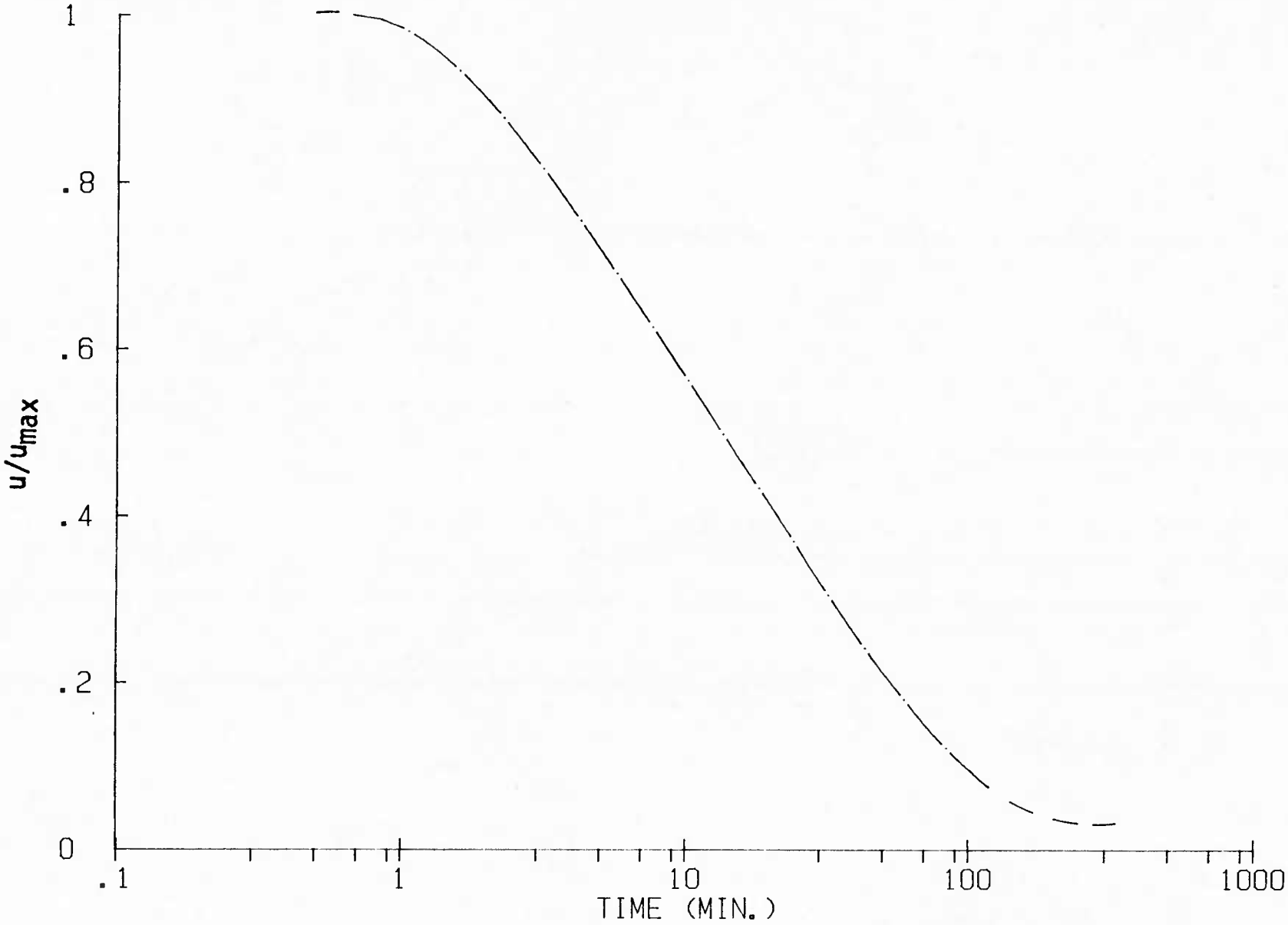

Figure 10. THE LOG (TIME) DISSIPATION CURVE FOR PROBE P-2

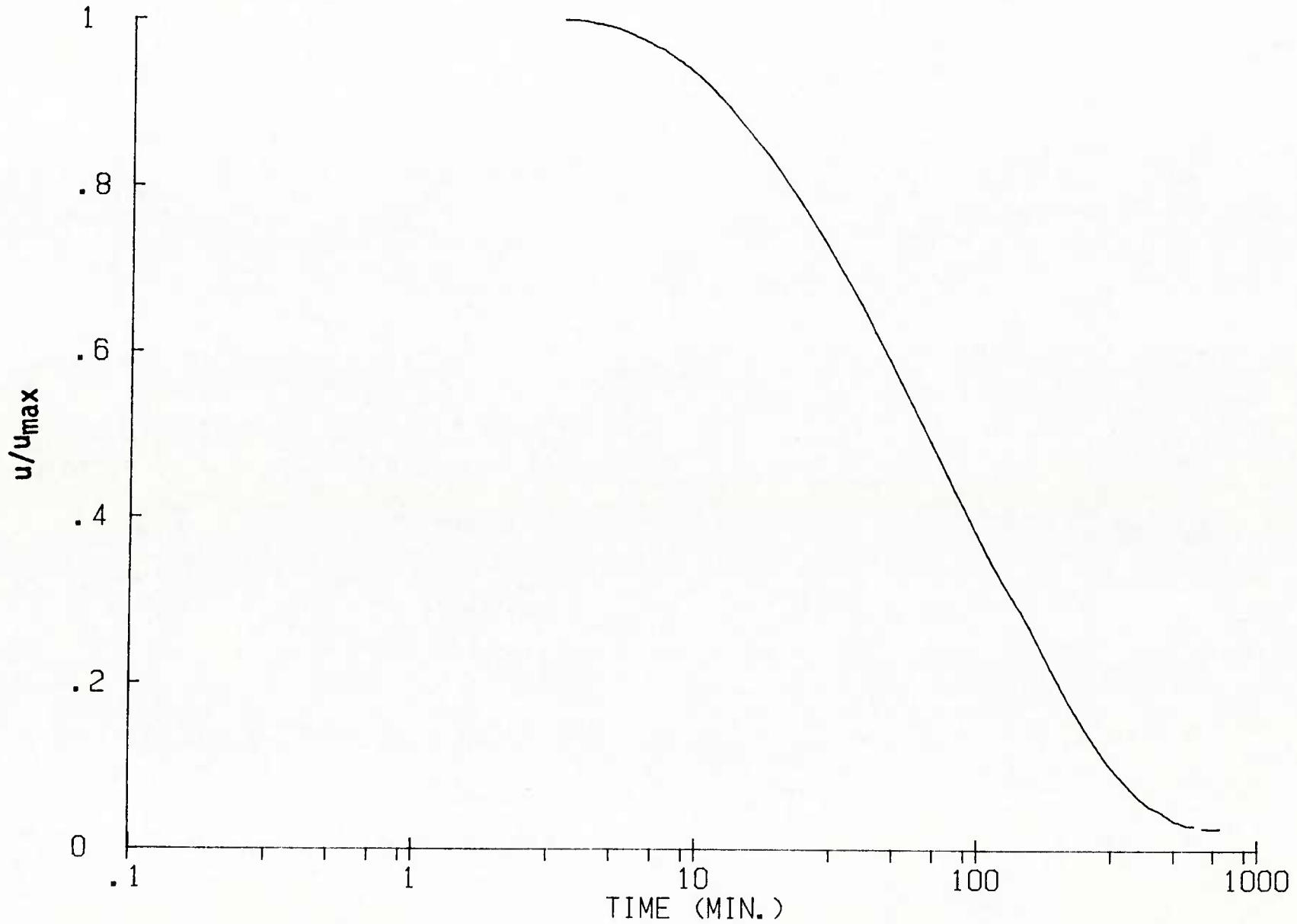

Figure 11. THE LOG (TIME) DISSIPATION CURVE AT PROBE P-3 DUE TO THE INSERTION OF HEATER PROBE

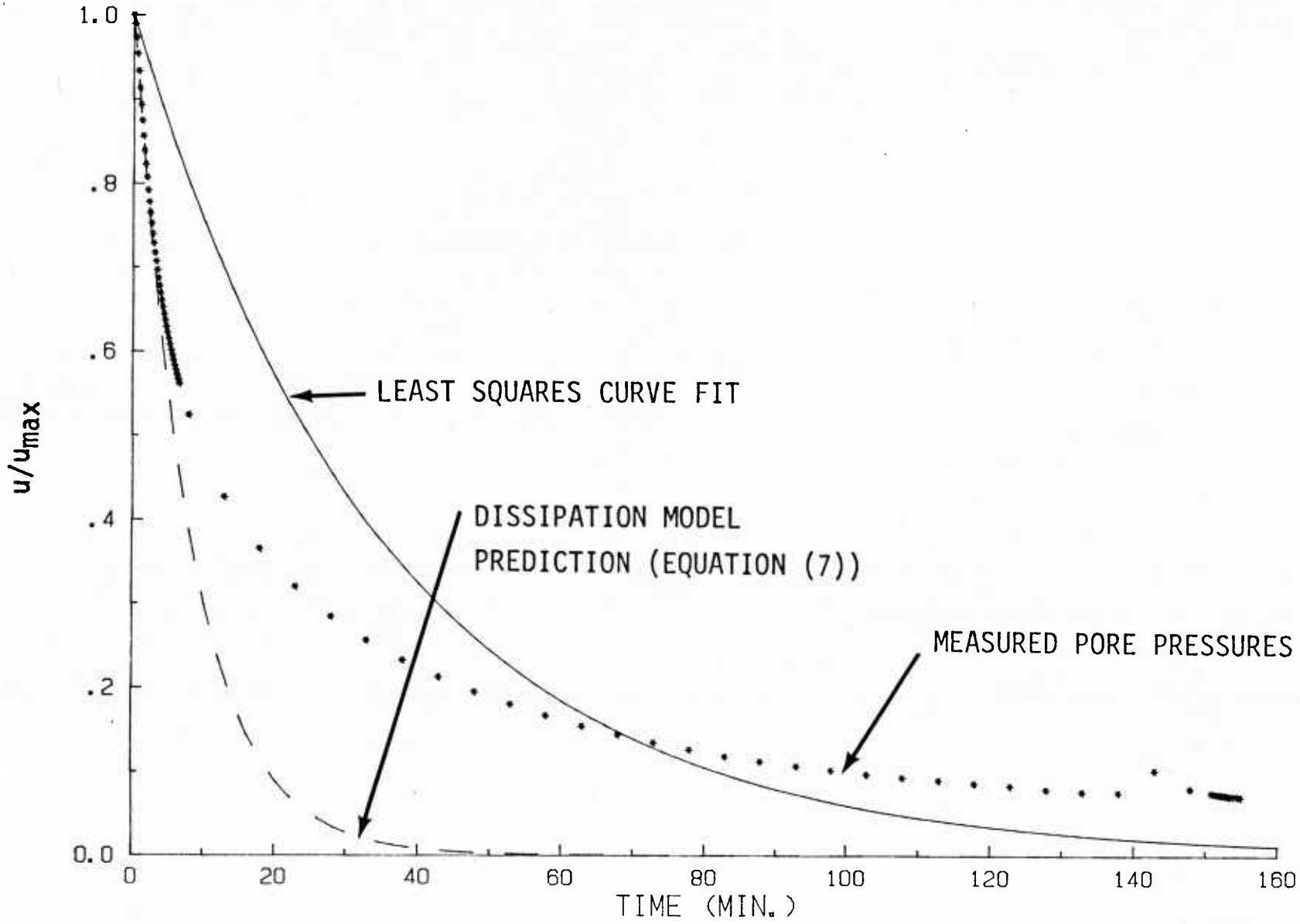

Figure 12. THE DISSIPATION CURVE AT PROBE P-3

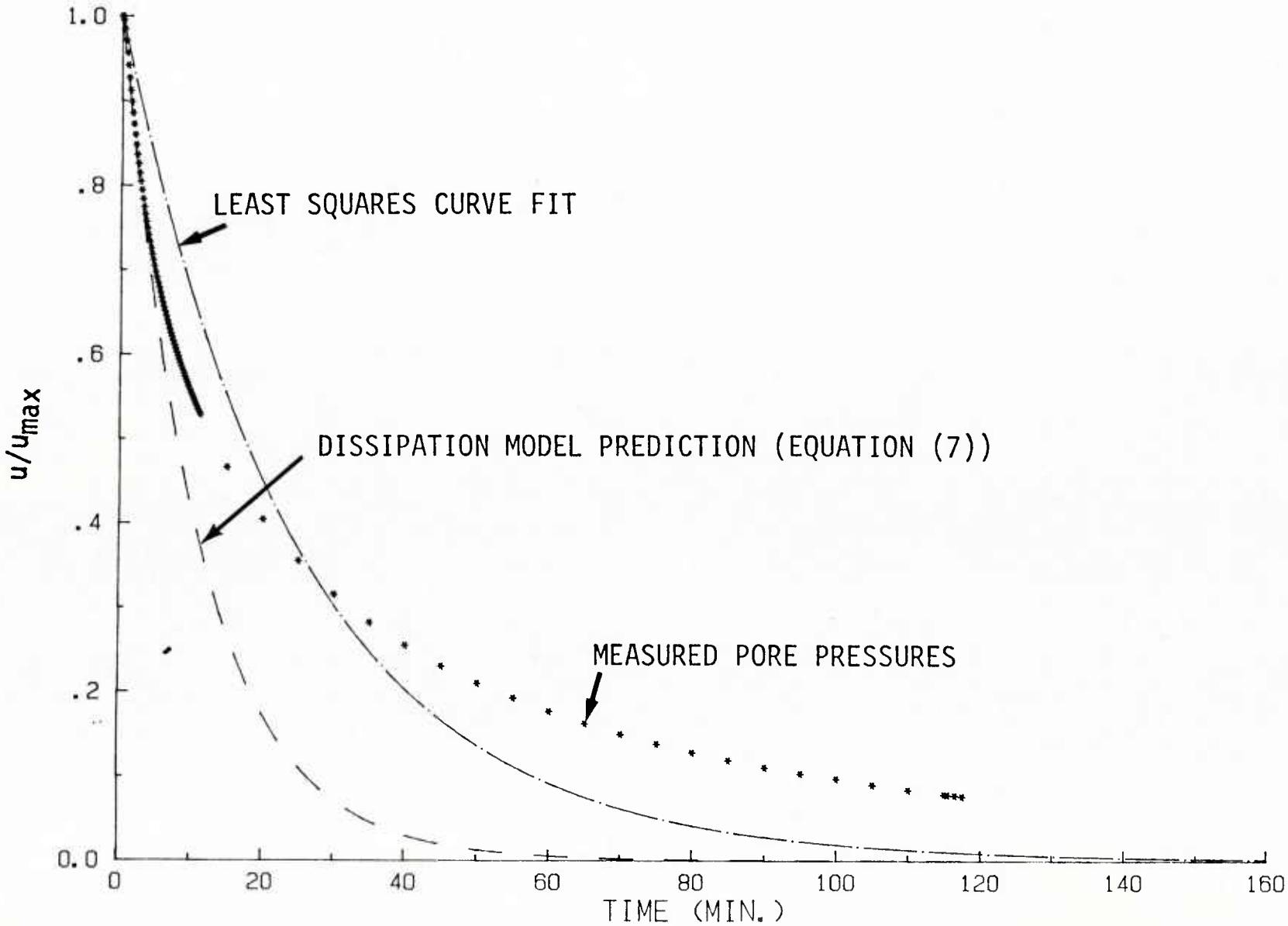

Figure 13. THE DISSIPATION CURVE AT PROBE P-2

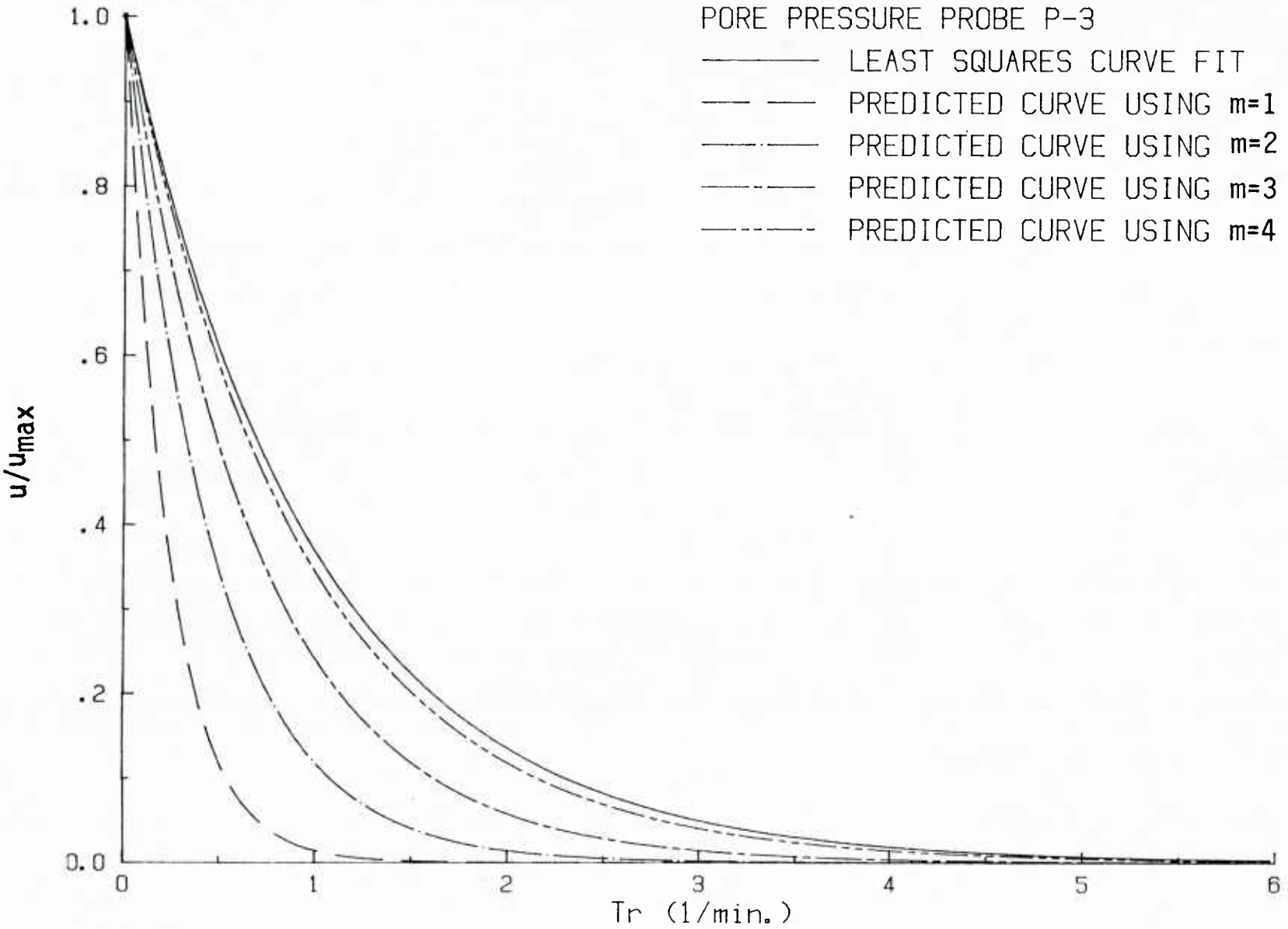

Figure 14. THE PREDICTED DISSIPATION CURVES AT PROBE P-3 AS A FUNCTION OF THE SMEAR FACTOR, m

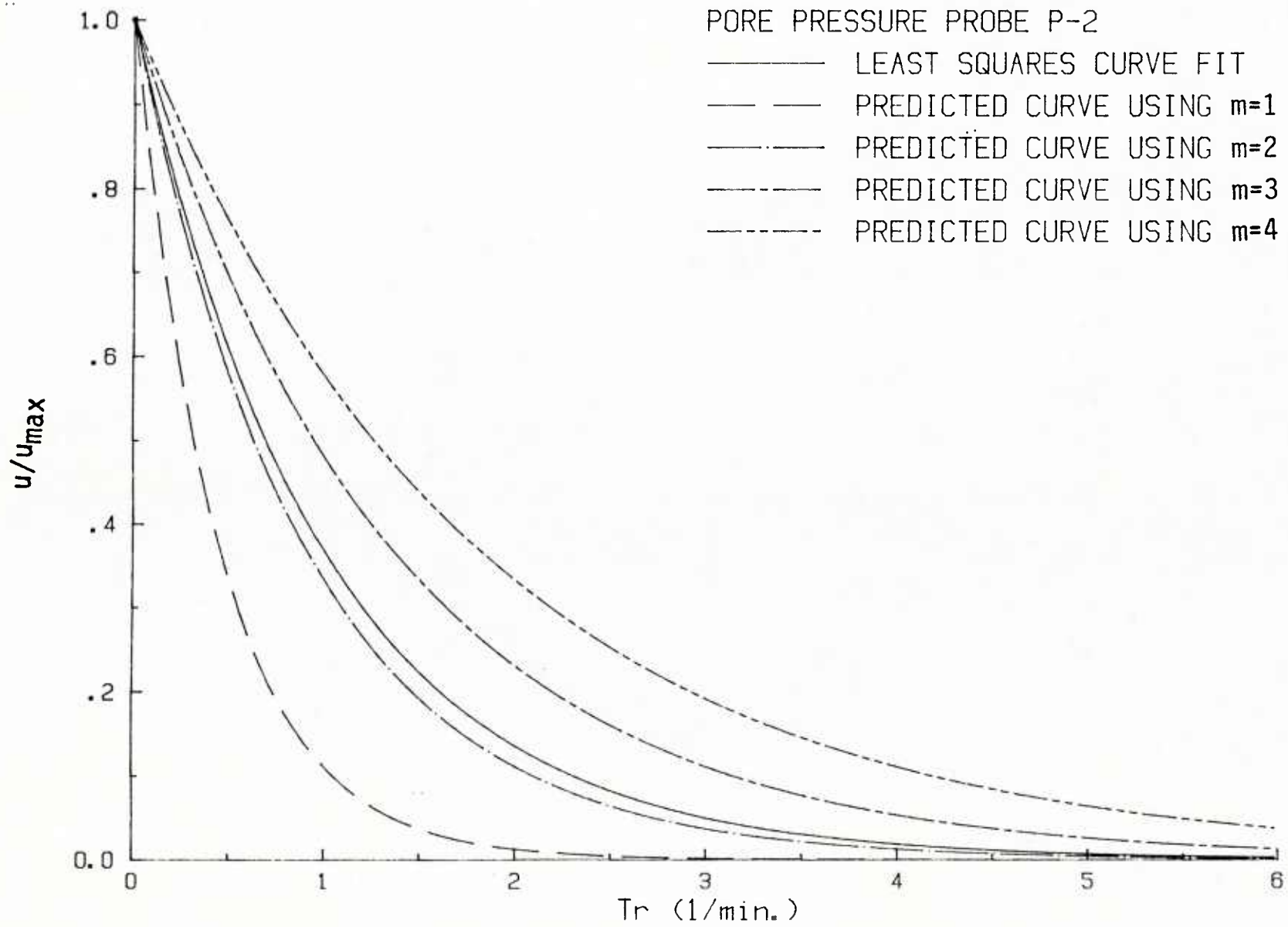

Figure 15. THE PREDICTED DISSIPATION CURVES AT PROBE P-2 AS A FUNCTION OF THE SMEAR FACTOR, m

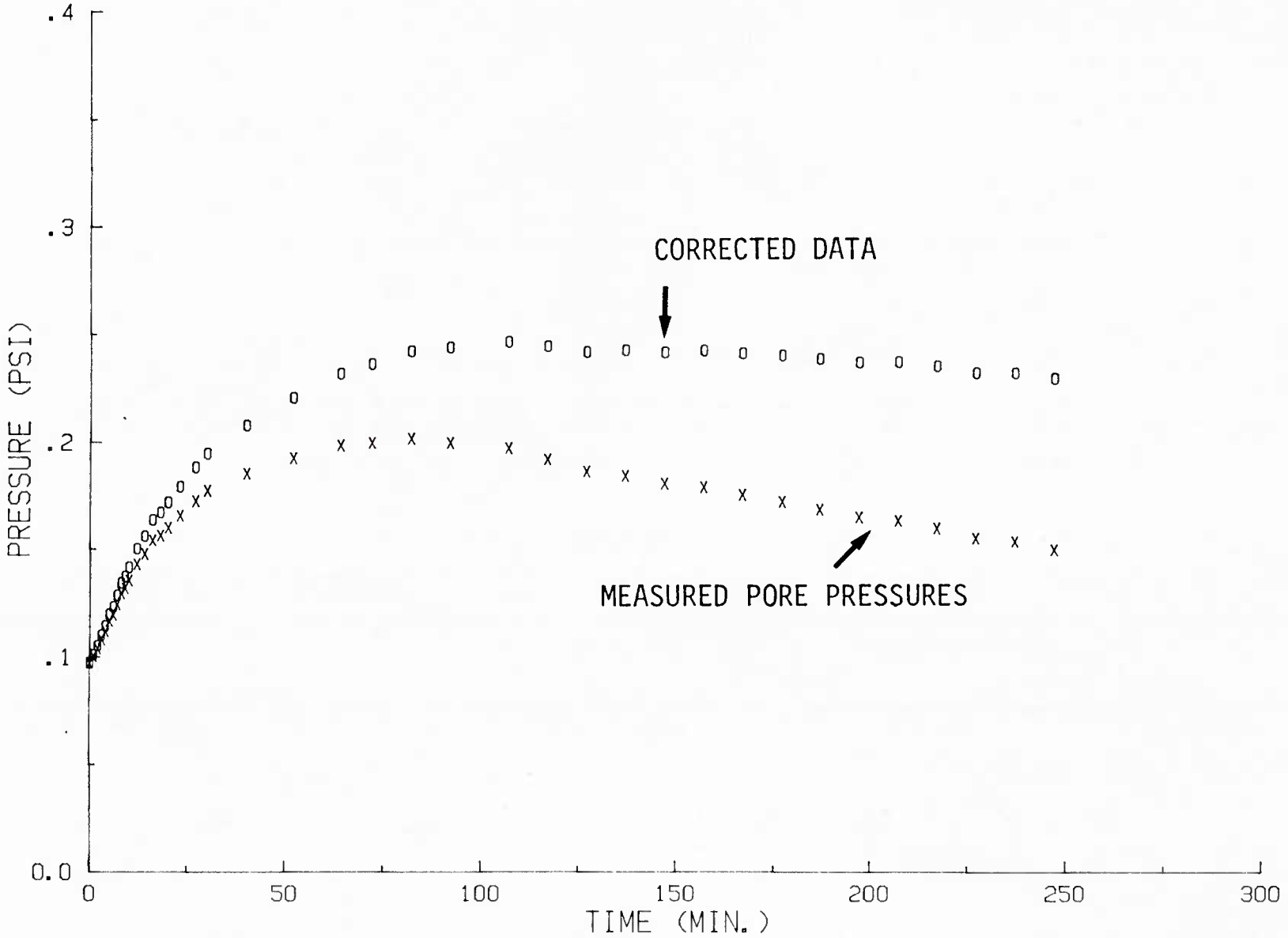

Figure 16. HISTORY CORRECTION FOR THE THERMALLY INDUCED PORE PRESSURES AT PROBE P-3

(1psi = 6.895kPa)

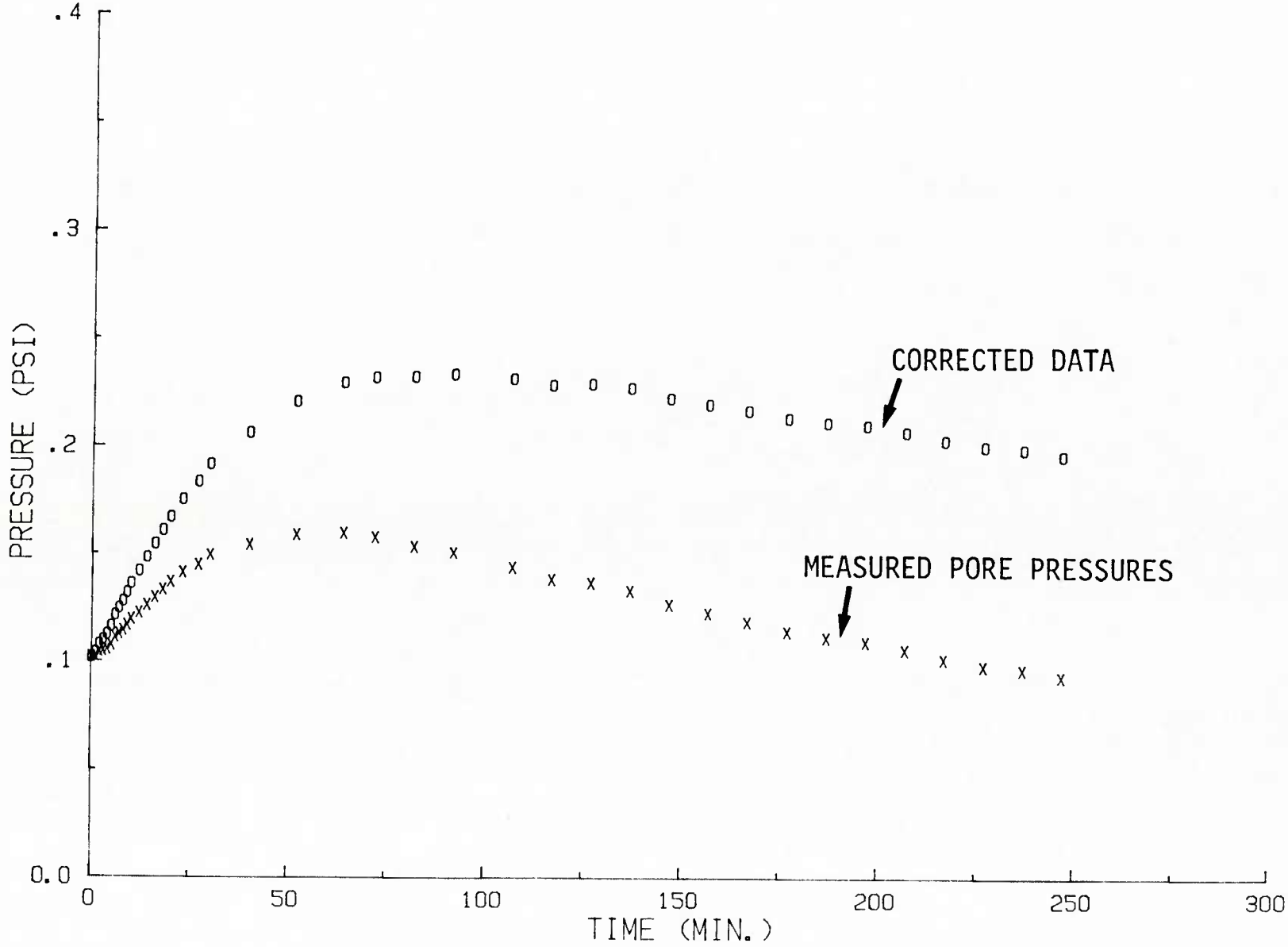

Figure 17. HISTORY CORRECTION FOR THE THERMALLY INDUCED PORE PRESSURES AT PROBE P-2

(1psi = 6.895kPa)

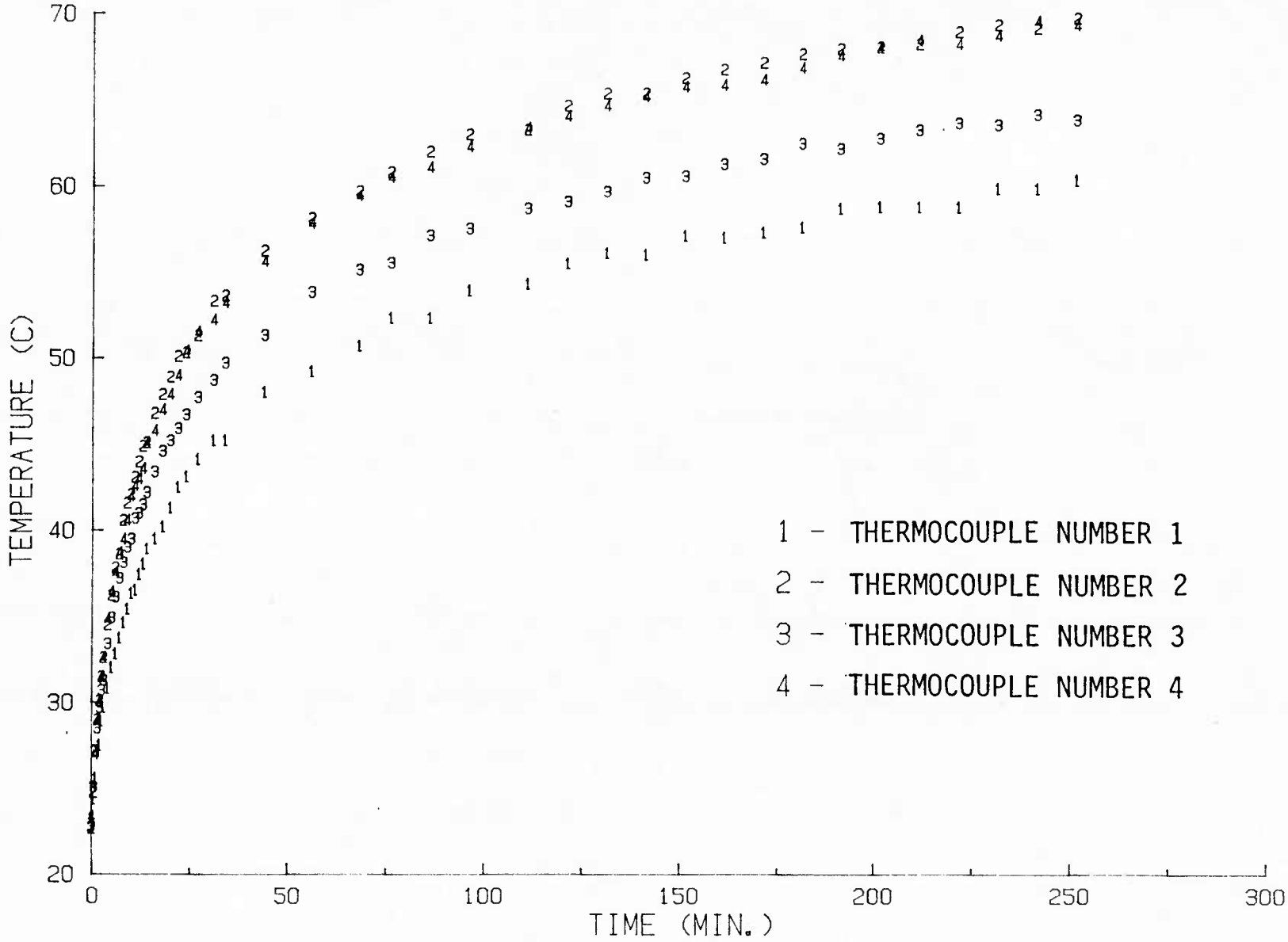

Figure 18. TEMPERATURE AT THE HEATING ELEMENT AS A FUNCTION OF TIME

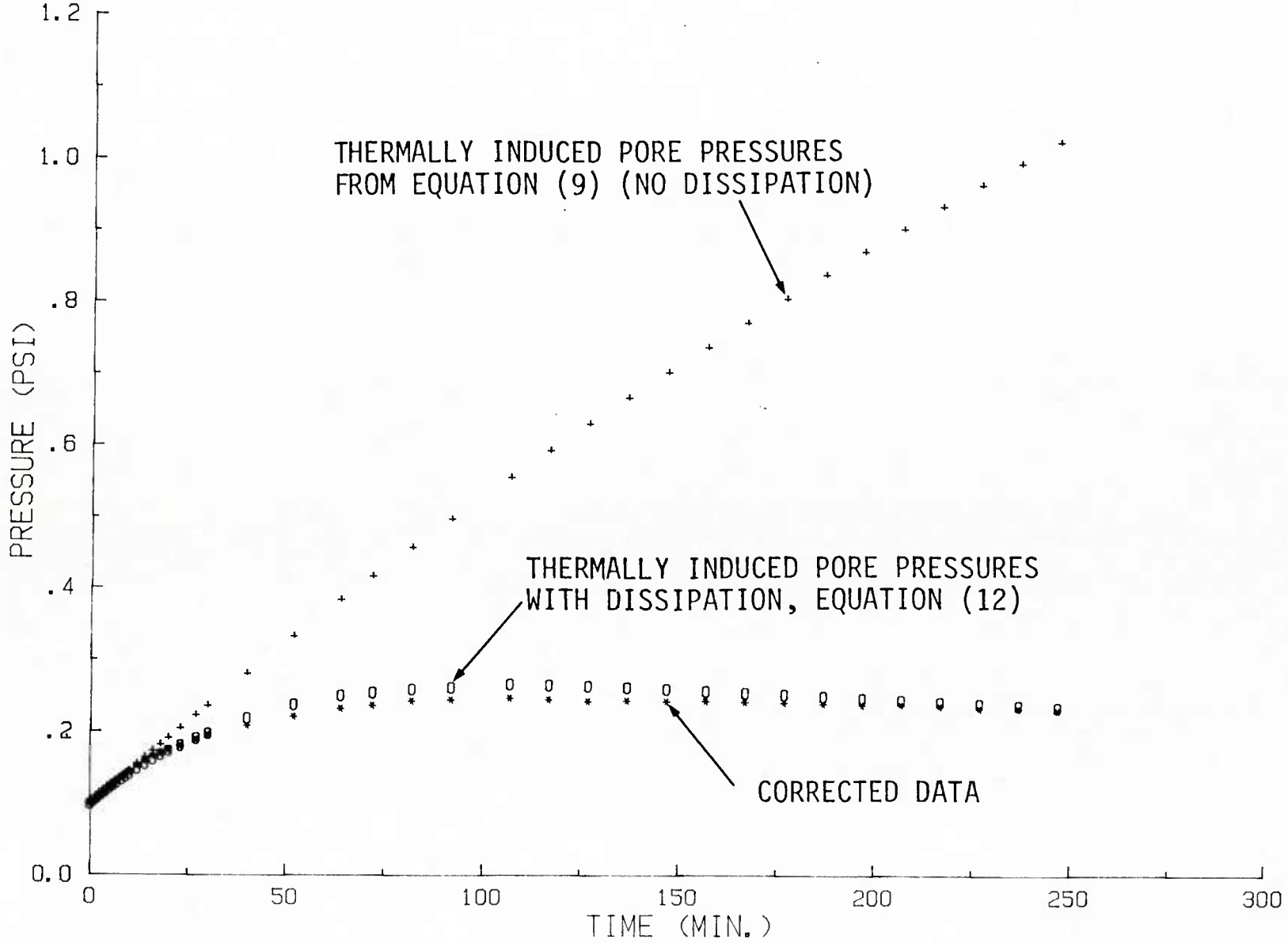

Figure 19. MODEL PREDICTIONS AT PROBE P-3 (1psi = 6.895kPa)

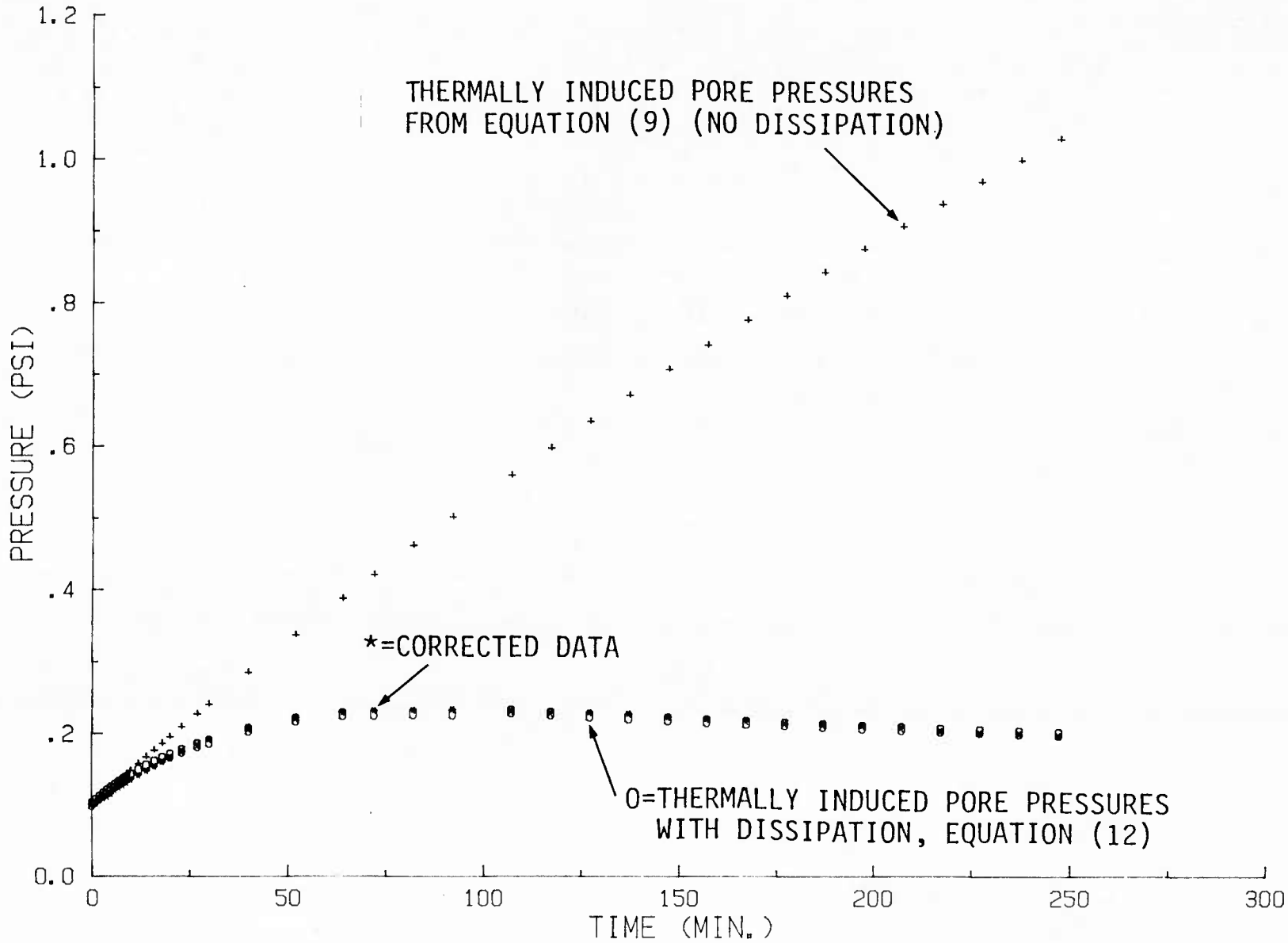

Figure 20. MODEL PREDICTIONS AT PROBE P-2 (1psi = 6.895kPa)

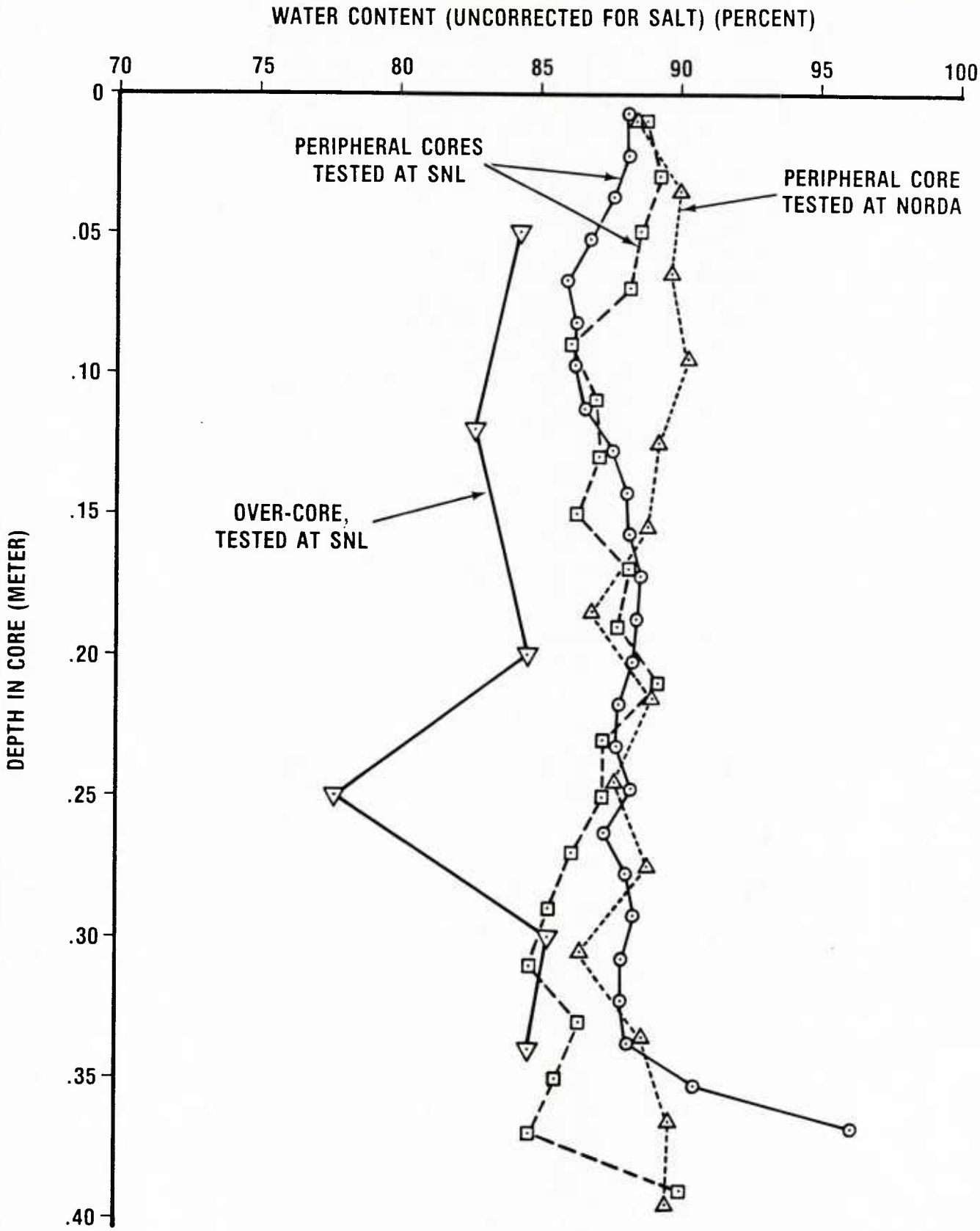

Figure 21. WATER CONTENTS OF TEST TANK SEDIMENTS AT CONCLUSION OF ISIMU-II EXPERIMENT

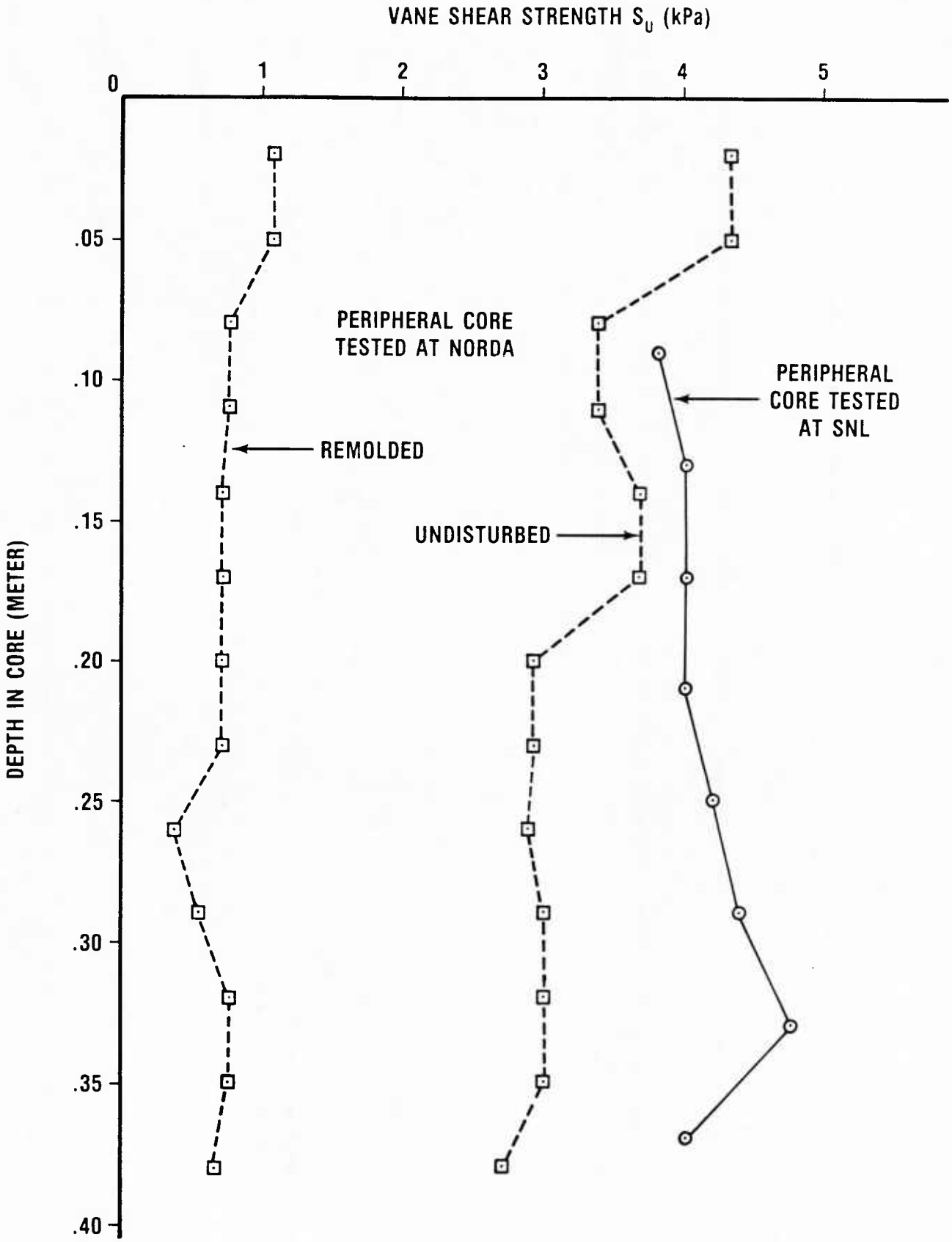

Figure 22. UNDRAINED SHEAR STRENGTHS OF TEST TANK SEDIMENTS AT CONCLUSION OF ISIMU-II EXPERIMENT